NASA CONTRACTOR REPORT

NASA CR-2234

NASA CR-2234

THE INFLUENCE OF DEFECTS AND IMPURITIES ON THE NUCLEATION AND GROWTH OF ORIENTED FILMS BY EVAPORATION

by A. K. Green

Prepared by
MICHELSON LABORATORY
China Lake, Calif. 93555
for Ames Research Center

NATIONAL AERONAUTICS AND SPACE ADMINISTRATION • WASHINGTON, D. C. • APRIL 1973

1 Report No	2 Government Accession No	3 Recipient's Catalog No
NASA CR-2234		

4 Title and Subtitle	5 Report Date
The Influence of Defects and Impurities on the Nucleation and Growth of Oriented Films by Evaporation	April 1973
	6 Performing Organization Code
7 Author(s)	8 Performing Organization Report No
A. K. Green	10 Work Unit No
9 Performing Organization Name and Address	11 Contract or Grant No
Michelson Laboratory Physics Division China Lake, California	NGR 05-030-001
	13 Type of Report and Period Covered
12 Sponsoring Agency Name and Address	Contractor Report
National Aeronautics & Space Administration Washington, D.C.	14. Sponsoring Agency Code

15 Supplementary Notes

16 Abstract

The influence of substrate imperfections on the Nucleation and Growth of fcc metals on alkali halides is discussed. Films deposited on well characterized substrates under well defined vacuum evaporation conditions are investigated. The experimental results of this work are correlated with similar work by other investigators. Models which have been proposed by various authors to explain experimental results are critically examined and areas of difficulty are pointed out.

The influence of defects on nucleation rate and the orientation of the film is emphasized. Specific examples of Impurity effects, Irradiation effects and the Influence of Amorphous layers are discussed in detail. Evidence is shown that the formation of Multiply Twinned Particles is a result of coalescence and growth. The only consistent model for the orienting influence of impurities is shown to be a chemical rea tion effect. It is demonstrated that an alkali metal impurity is very likely responsible for the orienting influence of both water vapor exposure and irradiation. A negative result is found for the reported possibility of an orienting influence being transmitted through an amorphous layer.

17 Key Words (Suggested by Author(s))	18 Distribution Statement
Thin Films Nucleation & Growth Epitaxy Vacuum Evaporation Impurity Effects	UNCLASSIFIED-UNLIMITED

19 Security Classif (of this report)	20 Security Classif (of this page)	21 No of Pages	22 Price*
UNCLASSIFIED	UNCLASSIFIED	41	3.00

*For sale by the National Technical Information Service, Springfield, Virginia 22151

TABLE OF CONTENTS

ABSTRACT

The influence of substrate imperfections on the Nucleation and Growth of fcc metals on alkali halides is discussed. Films deposited on well characterized substrates under well defined vacuum evaporation conditions are investigated. The experimental results of this work are correlated with similar work by other investigators. Models which have been proposed by various authors to explain experimental results are critically examined and areas of difficulty are pointed out.

The influence of defects on nucleation rate and the orientation of the film is emphasized. Specific examples of Impurity effects, Irradiation effects and the Influence of Amorphous layers are discussed in detail. Evidence is shown that the formation of Multiply Twinned Particles is a result of coalescence and growth. The only consistent model for the orienting influence of impurities is shown to be a chemical reaction effect. It is demonstrated that an alkali metal impurity is very likely responsible for the orienting influence of both water vapor exposure and irradiation. A negative result is found for the reported possibility of an orienting influence being transmitted through an amorphous layer.

1.0 INTRODUCTION

The work reported here is concerned with the growth of fcc metals on alkali halides. These systems have been used extensively for investigations of defect and impurity influences and therefore are the most appropriate for this topic. The growth is characterized by poor wetting of the substrate by the deposit and the formation of 3-dimensional crystallites in the nucleation stage of film growth. The growth mechanism has been referred to as the Volmer-Weber mechanism[1] because of their treatment of similar systems published in 1926.[2] The results discussed here are valid only for systems which exhibit the V-W growth mechanism.

The decoration of cleavage steps is the most obvious influence of defects on the formation of metal films evaporated on alkali halide cleavage surfaces. Figure 1 shows an example of a NaCl surface decorated with Au. This technique, as first demonstrated by Bassett,[3] has been very successful at revealing the microtopography of the cleavage surface. Bethge[4] has pursued this in detail and has provided an explanation in terms of the crystal defect structure for the observed decoration patterns. In Figure 1 we can clearly see linear features. Careful analysis of such linear features enabled Bethge to conclude that the emergence points of the edge dislocations of a tilt boundary were preferred nucleation sites. In between the line type decoration it is much more difficult to identify nucleation sites with defects. This is because the spatial distribution is random and only a careful study of the nucleation kinetics can distinguish defect from defect-free sites. The work of Robins,

Rhodin and Gerlach[5] with MgO substrates also demonstrates the resolution and sensitivity of the nucleation decoration technique for studying surface defect structure.

2.0 SUBSTRATE DEFECTS

2.01 Classification

We will not limit our discussion simply to the influence of crystallographic defects but will also consider impurity effects and irradiation effects. For the purposes of this paper, Figure 2 classifies the types of defects which may occur on the surface of alkali halide substrates.

A point imperfection is classified as a 0-dimensional defect. Vacancies, interstitials, F-centers, bulk impurity atoms, adsorbed atoms (of residual gas or substrate decomposition product) and the emergence point of dislocations are examples of 0-dimensional defects. Cleavage steps, slip planes which intersect the surface and tilt boundaries are considered as 1-dimensional defects. Surface layers are classified as 2-dimensional defects, e.g., adsorbed layers, reaction layers, and intentionally deposited amorphous layers. Precipitates are also considered as 2-dimensional defects. Because we are just concerned with surfaces, these classifications differ from the classifications in the bulk of a crystal where, for example, a grain boundary would be 2-dimensional and a precipitate would be 3-dimensional; on the surface of the crystal they are 1- and 2-dimensional, respectively.

2.02 Difficulties of Classification

An unequivocal classification of the defects produced is very difficult in most cases. For example, water vapor exposure of NaCl is known to result in the formation of hydroxides.[6] This could be in the form of a continuous or

discontinuous layer (2-dimensional), may exist only on steps (1-dimensional) or may even form only at specific sites (0-dimensional). Decoration of NaCl surfaces which have been exposed to water vapor by cleavage in laboratory air reveals the presence of both 1- and 2-dimensional defects. 0-Dimensional defects are also produced by water vapor exposure in vacuum after vacuum cleavage. The same difficulty in classification exists for any gas exposure whether reactions take place or simply adsorption.

Irradiation-produced defects also present difficulties in classification. Electron bombardment of alkali halides has been claimed to produce only F-centers.[7] However, this claim is very likely an oversimplification because of the experimentally observed buildup of alkali metal on the surface during bombardment. The alkali may be present in the form of randomly distributed atoms or in aggregates. Furthermore, the F-center-related vacancies may also form in aggregates. So a clear unambiguous classification of defects produced by irradiation is not possible at the present time.

The distribution of impurity atoms resulting from doping is also open to speculation. Point defects would exist if the dopant atom replaced an atom of the host material or assumed an interstitial position. Accumulation of dopant along a planar defect in the bulk would result in a 1-dimensional defect on a cleavage surface. Aggregates of impurities would result in 2-dimensional defects.

2.03 Production and Control of Defects

By proper choice of the substrate treatments, however, it is possible to control the defect structure of the surface to a limited extent. Experimentally, as already mentioned, the defect structure is best observed by decoration and

a correspondence between defects on one hand and nuclei density and distribution on the other hand is implicit. This correspondence is not simple and direct. The nucleation rate also depends on other parameters, for example, on the supersaturation which is a function of the deposition rate and the substrate temperature. Nucleation can also occur on defect-free sites. The most meaningful results obtained so far are comparative in nature. Two or more substrates as nearly identical as possible are used simultaneously. One is exposed to a specific treatment and the other is a control sample. The decoration procedure of evaporating less than 5 Å of metal is performed simultaneously on both samples under identical conditions.

The comparison of air- and vacuum-cleaved surfaces, as seen in Figure 3, is a typical example of the influence of air exposure on the defect structure of alkali halides. By cleaving in vacuum the nucleation density is usually decreased. This effect and its influence on film orientation will be discussed in detail later. Irradiation by electrons and x-rays have also been used to introduce defects. Figure 4 shows a comparison of results from an irradiated area and an unirradiated area of a vacuum-cleaved NaCl surface. Clearly, the irradiation effect has completely changed the defect structure of the surface. This complex phenomena, which can significantly affect the particle orientation as well as the distribution and density, will be discussed as a separate topic. Some other methods of controlling the defect structure are:

(1) Additively coloring the bulk crystal,

(2) prestressing the bulk crystal,

(3) doping the bulk crystal,

(4) exposing the surface to specific gases, and

(5) accelerating the ions in the depositing vapor beam.

2.04 Defects as Preferred Nucleation Sites

The theoretical treatment of the influence of defects on nucleation is limited. Cahn[8] in 1957 reported an analysis of the activation energy of nucleation of a second phase on a dislocation. This treatment used macroscopic thermodynamic quantities and the lower limit of validity claimed is for nuclei with 10 Å radius. This would mean ∿ 130 atoms in the nucleus and for the systems considered in this discussion is certainly too high. Rhodin and Walton[9] have derived an expression for the nucleation rate on point defects using their atomistic formulation. This has been modified by Frankl and Venables[10] but only very qualitative agreement with experiment has been achieved. Recently, a more comprehensive treatment has been given by Stowell and Hutchinson.[11] This analysis is an extension of Stowell's model of the nucleation process to include preferential growth sites. Comparison with experiment is not available at present.

Experimentally, it is found that the density of dislocations on the surface of alkali halides revealed by etch pit studies is much less than the observed nucleation density. For KCl, etch pit densities from 10^4 to 10^8 cm^{-2} have been observed[12] while observed nucleation densities are 10^{10} to 10^{12} cm^{-2}. When matched cleavage surfaces are used a one-one correspondence of etch pits is found. Stirland[13] has attempted to observe a correspondence between nucleation sites on matched cleavage surfaces using the decoration technique. At $T_s < 150°C$ there is a correspondence between steps but not between individual sites. Above 150°C even the step structure on both cleavage surfaces could not be correlated.

A correlation between the density of point defects estimated from impurity content and observed nucleation density of Au on MgO has been reported by Robins and Rhodin.[14] They claimed agreement within an order of magnitude

between the observed saturation density of $3.5 \times 10^{11} cm^{-2}$ and the surface impurity atom density for either the Fe^{+3} or Si^{+4} impurities. However, the density of the Fe and Si impurities determined from the lowest concentrations quoted are each $\sim 1 \times 10^{12} cm^{-2}$. Their MgO analysis also indicates CaO impurities of 0.15% which would produce an impurity density of $\sim 1 \times 10^{13} cm^{-2}$ on the surface. So the density of impurity atoms on the surface is at least two orders of magnitude higher than the observed saturation nucleation density. The implication of a one-to-one correspondence between impurity atom sites and nucleation sites is clearly misleading.

The influence of steps on nucleation has been discussed using macroscopic thermodynamic concepts in terms of the relative magnitudes of the various surface and interfacial energies involved[15] or in terms of contact angles.[16] Halpern[17] has treated decoration atomistically using an extension of his 2-dimensional random walk nucleation theory.[18] He concludes that a line defect will lead to a void border along the line with a width of one-half the diffusion length of a deposit atom on the substrate. A void border along steps is routinely observed with low evaporation rates for Au/NaCl on both air- and vacuum-cleaved surfaces. This is easily understood qualitatively, and results from the depletion of adatoms near the step due to the high density of nucleation sites along the step. The diffusion length of an atom on the surface is clearly the determining factor for the width of this border.

Qualitatively, the behavior of defects as nucleation sites is understood. Quantitatively, however, much work remains to be accomplished.

2.05 Orienting Influence of Defects

The enhanced frequency of nucleation on defects is unquestioned. The orienting influence of defects, however, is controversial. Palmberg et al.[19] have suggested that the defects on MgO are "tight-binding" sites which promote epitaxy. Ueda and Inuzuka[20] have reported that selective nucleation of epitaxial crystallites occurs on point defects. They arrived at this conclusion by comparing the observed nucleation density and orientation of Au on NaCl at 300°C as a function of deposition rate and thickness (< 1.0 Å). At very low rates (0.005 Å/sec and 0.04 Å/sec) they observed only (100) oriented particles. At higher rates (0.23 Å/sec) they observed multiply twinned particles and only very weak (100) orientation. These observations are consistent with our own work but we believe the results show that the orientation of the Au crystallites is rate-dependent--not that selective nucleation of epitaxial particles occurs on defects. Grünbaum and Matthews[21] studied the growth of Au/NaCl on heavily stepped compared to sparsely stepped surfaces with electron diffraction and with dark field microscopy. They concluded that steps did not significantly influence the orientation of Au nuclei. Bethge,[22] also using dark field microscopy, found no influence of either steps or the emergence points of dislocations on nuclei orientation.

In contradiction to these results are those of Sato and Shinozaki.[23] They have studied the particle shape and orientation of Au on NaCl at one temperature (275°C), one thickness (35 Å), and at estimated rates between 0.1 and 0.75 Å/sec. They observed epitaxial particles preferentially along steps and attributed the epitaxial orientation of the particles on steps to an increased interfacial energy resulting from the defect. The fact that their films were in the coalescence stage of formation (35 Å average thickness) and

that the rate effect was neglected makes any conclusions about nucleation events from their work very questionable. Chopra[24] has added to the confusion here by stating in his book that a defect-free surface will enhance the adatom mobility and improve the orientation. Because oriented particles are also observed on steps, Chopra concludes that defects do not alter the orienting influence of the substrate. Sato's conclusions are just the opposite, i.e., that the smooth substrate has no orienting influence and that the defect is responsible for the orientation.

Our own experimental observations have been limited to electron diffraction and bright field electron microscopy. However, our in situ reflection electron diffraction work is extremely sensitive to initial orientation and when coupled with electron microscopy has led us consistently to the conclusion that steps influence particle distribution and size, but not orientation. The most powerful techniques to study the orientation of individual particles have been developed by Poppa and Heinemann.[25] The lattice-imaging method is the most direct way and they have used this technique to determine not only the orientation of the epitaxial particle but have also precisely determined the azimuthal alignment of the particle. By imaging the lattices of both the deposit particle and the substrate simultaneously, the azimuthal angle can be determined within 1°. While this method is powerful it is severely limited for general use because of the difficulty of imaging lattice planes. Another very elegant technique developed by Poppa and Heinemann is the Bragg Reflex-Image method. This method uses the fact that a single crystal particle produces not only a bright field image but also a dark field image that is displaced from the bright field image by an amount depending upon the defocus of the objective lens and the specific diffraction angle. In general, by taking two

micrographs with a known defocus difference it is possible to determine the diffracting planes responsible for the "reflex" image. Figure 5 shows the result of this technique applied to a Au film which has decorated the steps of a vacuum-cleaved NaCl surface. The film was prepared in our lab and the micrographs taken by Heinemann. The bright field image on the left shows the typical step structure. The dark field image on the right is from the same area with approximately 500 nm defocus. The bright field image is taken with a normal objective aperture and the dark field image is taken with an annular aperture which blocks out the primary beam and allows the (111) and (200) diffracted beams to form the image. The images of nearly all of the particles in dark field are multiple and have expanded radially. This is typical for a multiply twinned particle with a (111) basis. Only the particles marked with an arrow are epitaxial. The particles marked with an elbow have not been studied sufficiently to be certain but very likely result from multiple twinning with a (100) basis. Clearly, in this case the steps have not produced epitaxial particles. The conclusion must be that steps on a vacuum-cleaved NaCl surface have not influenced the orientation of the deposited Au particles. The steps are preferred nucleation sites but do not by themselves determine the orientation.

3.0 IMPURITY EFFECTS

In this section we consider some specific examples of impurity effects. For this discussion the effect of intentionally contaminating a substrate surface prior to deposition will be emphasized. Except for our results on the influence of chlorine, we limit ourselves to growth in a clean vacuum on pretreated substrates.

3.01 Air Exposure (Water Vapor)

It is a well established result that Au will grow in uhv with parallel epitaxial orientation on a NaCl surface which has been cleaved in air but not on a NaCl surface cleaved in vacuum. Exposure of a vacuum-cleaved surface to water vapor produces results similar to air exposure; this implies that water vapor is the active component in air. Henning[26] has shown, in addition, that while water vapor is effective, a combination of H_2O and CO_2 is not. Figure 6 demonstrates again the typically reported differences for the very early stages of growth of a Au film deposited simultaneously on air- and vacuum-cleaved NaCl. The decoration features are completely different. Air exposure has removed the linear step structure and resulted in a surface with preferred nucleation sites concentrated in river-like bands. The average particle density on the air-exposed surface is $\sim 5 \times 10^{10}$ cm^{-2} and on the vacuum-cleaved surface is $\sim 7 \times 10^{9}$ cm^{-2}. The particle density on the flat areas is $\sim 7 \times 10^{9}$ cm^{-2} on both surfaces. The diffraction patterns show a predominant (100) epitaxial orientation on both surfaces. It must be emphasized that while these decoration features are characteristic for air- and vacuum-cleaved surfaces they are not typical for the entire surface. This is especially true for the vacuum-cleaved surface. The decoration pattern of Figure 6 represents usually no more than 20% of the entire vacuum-cleaved surface and in some cases cannot be found at all. A much more typical pattern from the same film is shown in Figure 7. Here the average particle density is nearly the same (5 and 2×10^{10} cm^{-2} air- and vacuum-cleaved, respectively) on both surfaces and on the flat areas the density is higher on the vacuum-cleaved surface (1 and 2×10^{10} cm^{-2} air- and vacuum-cleaved, respectively). A comparison of the vacuum-cleaved surfaces in these last two figures shows that the orientation

in the early stage of growth is the same on high particle density regions as it is on low particle density regions. It is also obvious that the orientation at this early stage of film growth is nearly the same on both the air- and vacuum-cleaved surfaces.

As mentioned before, we have found this to be a rate-dependent phenomena. At low rates ($\leq \sim 0.1$ Å/sec), as demonstrated here, the initial orientation is (100) with the multiply twinned particles and (111) forming during growth on the vacuum-cleaved surface. At higher rates, as seen in Figure 8, the multiply twinned particles and (111) are already observed at this early stage. Evidence for multiply twinned particles is present on both air- and vacuum-cleaved surfaces. The arcs on the (111) and (220) rings are characteristic for multiply twinned particles.

As the film grows thicker the orientation difference between air- and vacuum-cleaved surfaces increases as seen in Figure 9. At this exposure the orientation on the vacuum-cleaved surface exhibits strong multiple twinning and (111) with very weak (100) spots. The particles on the air-cleaved side have well developed square shapes at this growth stage. A still thicker film, as seen in Figure 10, continues the trend towards (111) fiber texture on the vacuum-cleaved surface and (100) parallel orientation on the air-cleaved surface. Notice the well developed crystal shapes on the air-cleaved surface and the fact that the orientation is as perfect on the flat area as on the high density river area. Figure 11 demonstrates the results for a continuous or nearly continuous film. One the air-cleaved surface the orientation has developed to completely epitaxial while on the vacuum-cleaved surface a two-degree (111) fiber texture is dominant.

As mentioned, this requirement for the existence of impurities to induce epitaxy has been explained in several ways. There is no doubt that the air or water vapor exposure produces an impurity layer. The composition of the layer and the way that it influences the film growth is still controversial. Harsdorff's model[27] is based on his claim that several layers of H_2O are adsorbed on the air-cleaved surface. He asserts that the adsorbed layers lower the substrate-metal interaction, which allows greater mobility and better orientation. Whether or not greater mobility leads to better orientation is controversial by itself and the reported evidence for adsorbed water layers has not been reproduced.[28] Adam[29] has reported the time dependence of the epitaxial influence of short water vapor exposures of elevated temperatures. The observed disappearance of the orienting influence can as easily be explained by the desorption or inward diffusion of NaOH as by the removal of H_2O layers. Sato[23] claims H_2O vapor increases interaction energy (less mobility) and leads to epitaxy in a manner similar to his argument about defects. Another mechanism, suggested by Matthews,[30] has been more favorably received and is often referred to as an explanation for orientation differences between air- and vacuum-cleaved surfaces.[31,32] This model is based on the observation that the average particle density is higher on the air-cleaved surface. Matthews assumes that the growth rate of (111) crystals is much larger than that of (100) crystals. Consequently, if a film contains both (111) and (100) particles which are far apart initially, the (111) particles will become larger than the (100) particles with increasing thickness. When coalescence occurs the smaller (100) particles will either recrystallize by diffusion or be converted into twins of the large (111) particles. If

coalescence occurs early because of a high particle density, then the (100) will dominate. The deciding factor for the final orientation according to this mechanism is the particle density. It is essential for this mechanism that both (111) and (100) particles exist in the very thin films, even for a film deposited at low rates and whose transmission electron diffraction patterns only show (100). Matthews claims that this is so and reports that dark field microscopy of 1 Å films reveals 10% of the particles are (111) in spite of the transmission electron diffraction pattern containing no spots from a (111) orientation.

There are several problems with this model.

1. Most of the (111) particles on the vacuum-cleaved surface do not have the flat shape assumed by Matthews but are multiply twinned particles. These particles are sphere-like rather than flat and the lateral growth would certainly not be faster than that of a (100) cube-like particle. This eliminates the basis of the mechanism.

2. The particle density in between the high density rivers on an air-cleaved surface is lower than the average particle density on a vacuum-cleaved surface but the particles in the coalescence stage on this low density area still develop (100) orientations in contradiction to the model.

3. Attempts to apply the model to other closely related systems, e.g., Ag/NaCl, Au/KCl and Ag/KCl are not successful.

Henning and Vermaak[32] have proposed a model to explain the frequently reported higher nucleation rate of (100) oriented particles on the water vapor exposed surface. They use a geometrical argument involving the radii of overgrowth atoms (r_o) and substrate nucleation centers and determine a critical radiums (r_{oc}) required for a perfectly accommodating (100) nucleation center in terms of the ionic radii of the substrate. If r_o is

less than r_{oc}, it is subcritical. The implication is that the nucleation rate in the supercritical case is higher than for the subcritical case. The difference in nucleation density on the air- and vacuum-cleaved surfaces follows from the difference in substrate ionic radii for a clean alkali halide surface (vacuum cleaved) and a hydroxide surface (air cleaved). Roos and Vermaak[33] have attempted to validate this model by studying thick layers of Au and Ag on NaCl, NaBr, NaF, KCl and KBr. The model predicts the final orientation in twelve out of twenty cases, if it is assumed that the particles retain their original orientation during growth and coalescence.

We have suggested another mechanism[34] based on the observation that air exposure of NaCl produces a hydrate-like surface layer[35,36] containing OH ions and possibly CO and CO_2.[37] Our mechanism attributes the differences between growth on air- and vacuum-cleaved surfaces to the coalescence stage. This mechanism asserts that upon coalescence the resulting particle assumes a configuration of the lowest free surface and interfacial energy which is attainable without considerable diffusion. If the anisotropy of surface-free energy does not change upon coalescence, and if the interaction between particle and substrate is weak, the resulting particle will have a tendency to be bound by {111} planes, including the contact plane with the substrate. Thus, the film tends towards a (111) orientation. If, however, during coalescence reaction between particle and substrate can occur, and if this leads to a lowering of the (100) surface and interfacial energy, the average film orientation will tend towards the epitaxial orientation. In applying this mechanism to the growth of Au on NaCl it is assumed that the air-cleaved surface can react with Au during coalescence. The impurities which react easily with Au, e.g., NaOH, are not present on the clean surface and the reaction does not occur.

Our model is compatible with the observations but requires that Au can react with the impurity layer and reduce the surface and interfacial energy of the (100) plane. Complimentary experiments using in situ reflection electron diffraction have provided evidence of such reaction products. A complete understanding of this mechanism and its extension to other systems requires knowledge of the chemical reactivity and the influence of reaction products on the surface and interfacial energy of specific planes.

The situation at the present time remains unclear. Each active group has its own apparently rather fixed ideas in spite of clear contradictions in some cases. All proposed mechanisms are open to question. Some have been shown to be clearly wrong while others have not been sufficiently proven.

3.02 Chlorine Exposure

One other extremely active gas for the epitaxial growth of Au and Ag on NaCl has been identified.[38] This gas is chlorine; in contrast to water vapor, chlorine must be present during the growth process for a positive effect on the orientation. Figure 12 demonstrates the influence of chlorine. These Au films were deposited under identical conditions, with the exception that a controlled chlorine leak maintained the pressure at 5×10^{-7} torr for the film on the right compared to 3×10^{-8} torr pressure with the chlorine leak closed. The film grown in the presence of chlorine has a higher coverage and is perfectly epitaxial as demonstrated by the transmission and reflection electron diffraction patterns. Figure 13 shows that chlorine is so effective at inducing epitaxy that it is possible to grow epitaxial films of Au on vacuum-cleaved NaCl at room temperature in a partial pressure of 5×10^{-7} torr Cl_2.

We believe that this is another example of an impurity effect where a surface layer has lowered the surface and interfacial energy of the (100) plane and induced epitaxy. The effect is not due to an alteration of the substrate surface because pre-exposure with chlorine is not effective. All results point to an influence on the growth and coalescence process. This is especially obvious for Ag on NaCl where the chlorine exposure can begin after 75 Å of Ag have been deposited and still be effective.

3.03 Doped Substrates

We now consider the published work in which intentionally doped substrates were used. Toth and Cicotte[39] have studied the influence of doping NaCl with calcium. The growth of Au and Ag on air-cleaved NaCl substrates with various concentrations of calcium chloride (200 ppm, 0.1 and 0.2 mole %) was compared to the growth on standard grade and high purity NaCl. They found that for temperatures above 450°C Au will grow epitaxially only in ultrahigh vacuum on the doped substrates. In normal vacuum (10^{-7} torr and poorer) and (111) texture predominates on the $CaCl_2$-doped NaCl. Similar results were found with Ag at a temperature of 250°C. In all cases, they observed higher particle densities on the doped substrates.

We have extended these experiments to include vacuum-cleaved substrates using 0.2 mole % Ca-doped NaCl obtained from Dr. Toth. As shown in Figure 14, the particle distribution is nearly the same on both doped and undoped vacuum-cleaved surfaces (undoped, 9×10^{10} cm^{-2}; doped, 5×10^{10} cm^{-2}). This demonstrates that the particle density influence found by Toth et al. is not from the doping by itself, but results from changing the interaction of the doped crystal with air. Figure 15 shows the effect of cleavage in air for a doped crystal. Here we see that the particle density

has increased and that the particle distribution is less uniform on the air-cleaved surface. An interesting feature is that contrary to the growth of Au on undoped NaCl, the orientation is definitely not improved by the presence of the impurity layer resulting from air exposure; this is in spite of the fact that the particle density is increased.

Birjega and co-workers[40] have studied the growth of Au films on NaCl doped with 7.5×10^{-3} mole % Ag. They deposited Au simultaneously on air-cleaved surfaces of pure NaCl, Ag-doped NaCl and electrolytically colored Ag-doped NaCl. Their results showed that at 200°C Au grew epitaxially only on the Ag-doped NaCl which had been electrolytically colored. The electrolytic coloration is claimed to produce colloidal Ag particles $\sim$ 100 - 200 Å. These authors do not speculate on a specific mechanism responsible for the induced epitaxy. The colloidal Ag particles may be oriented (Cl_2 influence) and be responsible for the orientation.

Sokol and Kosevich[41] have studied the influence of metallic Na and Li on the growth of Au on additively colored KCl and NaCl. They placed the alkali metal into holes drilled in KCl and NaCl and then heated the crystal to diffuse the alkali into the crystal, producing a concentration gradient. Cleavage of the crystal exposed a surface which they describe as containing three zones of different color, depending on the distance from the alkali metal source. For Na they observed epitaxial growth of Au within these diffusion zones of both air- and vacuum-cleaved NaCl. For Li they found improved orientation on an air-cleaved surface. We will have more to say later regarding the enhancement of epitaxy by the presence of an alkali metal.

While the MgO used by Robins and Rhodin[14] was not intentionally doped, it contained a significant concentration of impurities. It was already

mentioned that a one-to-one correspondence between impurity atoms and nucleation density does not occur in this case. In fact, we have compared the growth on standard optical quality MgO as used by Robins with the growth on high purity, specially prepared MgO and found no significant difference. The high purity MgO was obtained from the Research Materials Division of the Oak Ridge National Laboratory, and was > 99.975% pure compared to a nominal 99.5% for the optical quality.

Obviously, the situation is not understood at the present time. The work so far has been of a one-shot nature and results are largely inconclusive. A systematic effort using different dopants and various film substrate combinations under well defined conditions will be required before any general statements can be made.

4.0 INFLUENCE OF IRRADIATION

A considerable amount of work has been done concerning the influence of irradiation of alkali halide substrates on the growth of deposited metal films. Most of the investigations have involved electron irradiation. Some work has been done with x-rays and some with accelerated ions.

4.01 Electron Irradiation

Electron irradiation during the growth of Au on NaCl produces epitaxial Au under conditions that would ordinarily not permit epitaxy.[42,43] Figure 16 demonstrates this effect. In this deposition the specimen was cleaved in vacuum, then one area was irradiated for 15 sec with a 15 kV beam of $\sim$ 1 μA cm^{-2}, the beam was turned off for 30 sec and moved to another area. At the end of the 30 sec wait the beam was turned on and the shutter opened simultaneously to expose the entire surface to Au vapor and one area to both electron irradiation and Au vapor. The electron beam was turned off after 15 sec and the shutter closed after 30 sec.

As seen on the right, the orientation is nearly perfect (100) epitaxy for the Au film deposited with the electron beam on during the first 15 sec of deposition. The orientation is predominantly (111) and multiple twinning on both the nonirradiated and preirradiated surface. The particle distribution is also considerably altered both by the simultaneous irradiation and by the preirradiation. The particle density is significantly increased by both simultaneous irradiation and preirradiation.

Continuous films grown under the same conditions are epitaxial on the simultaneously irradiated area and have a (111) fiber texture on both the nonirradiated and the preirradiated surfaces. Similar results from simultaneously irradiated and nonirradiated surfaces are obtained with KCl, KI, KBr and LiF. A significant difference observed between the different systems is that preirradiation is effective in inducing epitaxy for both KBr and LiF. In fact, for LiF we have observed that the beam influence was still present after a waiting period of three weeks. The irradiation (two min at $\sim$ 1 $\mu A\ cm^{-2}$) was performed at 200°C in a vacuum of 1×10^{-9} torr and the specimen then cooled to room temperature. After three weeks the specimen was heated again to 200°C for the deposition. The preirradiated area exhibited predominantly (100) epitaxial Au while the nonirradiated area produced (111) and multiple twinning.

Generally, the experimental results of various workers on the influence of electron irradiation on epitaxy are quite consistent. However, different models have been proposed to explain the observations. The suggestion by Stirland[44] that the effect results from changes at the substrate caused by irradiation goes unchallenged. Rhodin and co-workers[7] have been more specific and developed a model based on preferred nucleation at single atom vacancies produced by the irradiation. This model is shown schematically in Figure 17. (a) Shows

the atomic positions of a NaCl surface with a Cl atom vacancy filled with a Au atom; (b) shows a four-atom Au nucleus formed at the Cl vacancy; (c) shows the configuration if a fifth Au atom is added; and (d) shows the minimum potential energy configuration claimed by Rhodin for the five-atom nucleus. The argument is very qualitative because the forces between the substrate and adsorbate are not well enough understood. Their justification for the correctness of configuration (d) is that a (100) oriented film develops. Stirland[45] has pointed out that if this model were correct the most likely configuration would be as shown in (e). This is 45° rotated from the epitaxial azimuthal alignment and is not observed.

While Rhodin's model is appealing because of its simplicity and apparently direct approach, it ignores evidence of the very complex phenomena that has been observed. We[43] have studied the formation of Au films on NaCl with *in situ* reflection electron diffraction and have found direct evidence of Au-Na compounds. Figure 18 illustrates the development of (100) oriented $NaAu_2$ during the irradiation of a thin Au film. We have also determined that a perfectly epitaxial Au film is formed if a continuous film is deposited on top of the $NaAu_2$ compound without additional electron bombardment.

The reflection electron diffraction pattern obtained *in situ* from all (100) epitaxial Au films exhibit 1/5th streaks. These 1/5th streaks can be interpreted as arising from double scattering between a layer with a $NaAu_2$ structure and the (100) Au surface. Palmberg and Rhodin,[46] and somewhat later, the group at the University of York--Prutton, Gallon, and co-workers[47]--have investigated alkali halide surfaces with Auger electron spectroscopy, mass spectrometry and low energy electron diffraction. Both groups observed time-dependent stoichiometry changes during electron irradiation leading to an

alkali-rich surface layer. Dissociation, sputtering and desorption occur with irradiation by electrons of energy above 100 eV. The crystallographic order and the impurities at the surface depend on the alkali halide, the way in which it was made and its treatment.

Lord[48] has used shadowed replicas to correlate growth sites with surface features produced by electron irradiation. He studied Ag on NaF and observed preferred growth of epitaxial Ag on substrate areas pitted by irradiation. He suggested that the preferred growth sites and enhanced orientation occurs on Na-rich areas.

Gallon and co-workers[49] have reported that simultaneous irradiation and deposition of Ag on KCl resulted in K diffusion over the Ag deposit and suggest that this would lead to the formation of interfacial alloys.

Recent work by Lad[50,51] has provided additional evidence, using Electron Paramagnetic Resonance, that electron irradiation of alkali halides produces free alkali metal. They have studied both LiF and NaCl. They find that a constant Li signal is observed in the spectrum from an irradiated LiF sample for at least a week after irradiation. For NaCl, however, the Na peak decays rapidly after irradiation (the vapor pressure of Na is $\sim 10^6$ times that of Li at 200°C). This is the same time dependence which we find for the influence of irradiation on Au films grown on NaCl and on LiF. This agreement between the lifetime of free alkali metal after irradiation and the influence of irradiation on epitaxy is another strong argument for the alkali metal being responsible for the orientation improvement.

4.02 X-Ray Irradiation

X-rays have also been used to irradiate alkali halide substrates. Inuzuka and Ueda[52] have reported that epitaxy is induced by x-ray irradiation of bulk NaCl

substrates. The specimens were preirradiated with CuK_α for five hr, then placed in the vacuum system and cleaved prior to deposition. They observed a higher particle density and predominant (100) orientation of a 10 Å Au film deposited at 80°C. Distler[53] also reports an increased particle number and improved orientation as a result of x-ray irradiation for Au on NaCl. We have tried repeatedly, without success, to reproduce these claims. Our results indicate absolutely no orientation influence and little, if any, particle density influence. Our conclusion is that F-centers by themselves do not influence orientation and that the effect observed by Inuzuka must result from a combination of F-centers with some other parameter.

There is one other reported influence of F-centers on film growth. Forssell and co-workers[54] have used additively colored KBr, KCl and NaCl substrates. They observed that at temperatures above 200°C Au films grown on the additively colored crystals exhibited a higher particle density and improved orientation. This effect was enhanced at higher temperatures and apparently not observed at lower temperatures. This temperature dependence would be consistent with colloid formation. Scott and co-workers[55] have shown that additively colored crystals form colloids with moderate heating. This suggests that a surface formed by cleaving a hot additively colored crystal would contain aggregates of free alkali. The surface defect responsible for the higher nucleation density and the improved epitaxy is very likely the alkali metal and not the F-centers.

4.03 Ion Irradiation

It has been observed by Mihama and Tanaka[56] and confirmed by our own work,[43] that acceleration of the ions in the depositing vapor beam will produce a

result similar to electron irradiation. Figure 19 illustrates the effect of placing a screen with -2.5 KV potential in the vapor path. Similar effects have been observed by depositing high energy ions,[57,58] sputtering[59] and by using a Knudsen cell at high positive potential.[43] This enhancement of orientation in all these cases can be explained with the same mechanism as suggested for electron irradiation. Enhancement of orientation and coalescence by a transverse electric field has been reported by Chopra[60,61] and more recently by Murayama.[62,63] This effect cannot be explained in terms of surface damage resulting from energetic particles. The transverse field effect has been explained as an influence of charged particles on the coalescence process. It is believed that charged particles would inhibit coalescence and that the transverse field would remove the charge and produce early coalescence.

It is clear that defects produced by irradiation have a significant effect on film growth. The nucleation density is definitely increased by irradiation but this by itself does not induce epitaxy. Atomistic models to explain the preferred orientation are not satisfactory. We believe that an impurity-controlled surface energy argument is the only consistent mechanism which will explain the experimental observations. During the coalescence process the impurity forms a reaction layer which lowers the surface and interfacial energy of the (100) surface. For Au on NaCl the reaction compound is $NaAu_2$ as observed by *in situ* reflection electron diffraction. This mechanism can also be used to explain the difference in growth on air-cleaved and vacuum-cleaved surfaces.

5.0 INFLUENCE OF AMORPHOUS LAYERS

Distler and co-workers have published a number of papers[64-66] attempting to establish a very controversial phenomena. Basically, the claim is that the surface of a single crystal substrate can be covered with an amorphous layer without impeding its epitaxial influence. Obviously, this claim is very pertinent to any discussion of the influence of the interface on film growth. We will briefly review the current situation and report the results of our attempt at reproducing it. The explanation of this reported effect by Distler and co-workers is a long range force which is transmitted through the amorphous layer. The amorphous layer is assumed to have replicated the same orienting influence which characterized the single crystal substrate. The long range forces are assumed to result from electrically active centers in the single crystal substrate. Barna and co-workers[67] have also reported this effect and claim that the amorphous layer forms an intermediate dielectric layer which replicates the effective surface potential field of the single crystal substrate. They claim that the layer acts as an electret and that the electrical forces at its surface are identical to those at the single crystal substrate and will induce epitaxy in the same way.

We will specifically consider two of Distler's papers. Both report results for PbS-C or SiO-NaCl. One published in 1967[65] and one published in 1971[66] have significantly identical contents. However, the maximum thickness used for the intermediate carbon layers decreased from 400 to 70 Å in the five-year period. The thickness of the layer now claimed and the temperature of the substrate during deposition (> 300°C) make the possibility of holes in the intermediate layer which expose the single crystal substrate very possible.

Figure 20 shows some results which we have obtained for the system PbS on NaCl with a SiO intermediate layer. The parameters were chosen to reproduce Distler's as closely as possible. In the left column we see just the SiO film with thickness of 20, 40 and 80 Å as monitored by a quartz crystal. These films were not self-supporting and were stabilized with carbon. The center column shows 40 Å PbS films deposited on top of the corresponding SiO film. The right column shows transmission electron diffraction patterns of the PbS films. The porous island structure which decorates the NaCl surface is clearly evident in the SiO film. The PbS films grow quite differently on different areas of the surface. Large agglomerated particles are typical of growth on a bare NaCl surface. The higher density and smaller particles are apparently on the SiO-covered surface. The effect of increasing SiO thickness on orientation is clearly seen in the transmission electron diffraction patterns.

Figure 21 shows the results obtained by using both air- and vacuum-cleaved NaCl and putting down a thicker PbS film. We used 80 Å PbS because we have found that an 80 Å film on bare NaCl is completely continuous. There is no significant difference between the results on air- and vacuum-cleaved surfaces. The films are composed of a jumble of cube-like particles completely randomly oriented.

Chopra[68,69] has made a systematic effort to reproduce this effect without success. Chopra's conclusion was that epitaxy can only occur on the exposed single crystal surface. Hayek and Schwabe[70,71] have attempted to resolve the problem. They find that films of C below 10-12 Å deposited on NaCl at 250°C contain holes as revealed by Ta-W shadowing and that above 10-12 Å thickness the Distler effect disappears. Hayek and Schwabe evaporated C from two or

more directions which would eliminate most of the shadowing effects and may account for the lower thickness of the amorphous layer at which they found the orienting influence to disappear. For SiO they have found that at substrate temperatures of 250°C the SiO layer is porous up to 50 Å thickness. Henning[72] also investigated the phenomena (Au-C-NaCl) and found that on vacuum-cleaved surfaces the Distler effect could be reproduced but not on an air-cleaved surface. This can also be understood in terms of holes in the amorphous layer if carbon, like many other materials, has a lower condensation coefficient on the vacuum- than on the air-cleaved surface of NaCl. The amorphous film formed on vacuum-cleaved NaCl would then have more island structure and less average thickness than the same thickness exposure on an air-cleaved surface.

The prospect of the orienting influence of a single crystal substrate being transmitted through a continuous amorphous layer is certainly exciting and, if true, would have a profound effect on the view of epitaxy. However, considering all the published and available reports, it seems very likely that the effect is not real.

6.0 SUMMARY

Table I summarizes the influence of defects and impurities for the nucleation stage of Au on NaCl. This system is used because it has been the most thoroughly studied. In cases of controversy our own results are used. The difficulties in classification, as mentioned before, must be kept in mind. For example, vacancies may be aggregates and if so would be more properly classified as 2-dimensional.

A similar table would be appropriate for the coalescence stage, with the exception that adsorbed layers can have a positive influence on both number

and orientation. The following conclusions stand out from the results reported here:

1. Neither the density nor the orientation of the initially formed particles have a determining influence on the final orientation.
2. The particle density on the flat surfaces of air- and vacuum-cleaved NaCl is the same but the final orientation is very different.
3. Multiply twinned particles form in the early coalescence stage and their formation as a function of thickness is rate dependent.
4. Specific impurities such as alkali metals and Cl_2 play a dominant role in the film orientation.

Clearly, there are many difficult and interesting problems that remain unsolved. Systematic experiments under very carefully controlled conditions are necessary to solve these problems.

ACKNOWLEDGMENTS

The author acknowledges, with pleasure, the significant contribution of his co-workers to the work reported here, especially to Prof. Ernst Bauer for his motivating influence and assistance. A special recognition is also due to John Dancy for his expertise with the electron microscope.

REFERENCES

1. Ernst Bauer, Z. Krist. 110, 372 (1958).
2. M. Volmer and A. Weber, Z. Physik. Chem. 119, 277 (1926).
3. G. A. Bassett, Phil. Mag. 3, 1042 (1958).
4. H. Bethge, Phys. Stag. Solidi 2, 3 (1962); ibid 2, 775 (1962).
5. J. L. Robins, T. N. Rhodin, and R. L. Gerlach, J. Appl. Phys. 37, 3893 (1966).
6. R. A. Lad, Surf. Sci. 12, 37 (1968) and references quoted therein.
7. T. N. Rhodin, P. W. Palmberg, and C. J. Todd, Molecular Processes on Solid Surfaces (1969).
8. J. W. Cahn, Acta Met. 5, 169 (1957).
9. T. N. Rhodin and D. Walton, Metal Surfaces, ed. by W. D. Robertson and M. A. Gjostein (Am. Soc. for Metals, Ohio, 1963), p. 259.
10. D. R. Frankl and J. A. Venables, Adv. in Phys. 19, 409 (1970).
11. M. J. Stowell and T. E. Hutchinson, Thin Solid Films 8, 411 (1971).
12. M. Sakamoto and S. Kobayashi, J. Phys. Soc. Japan 13, 800 (1958).
13. D. J. Stirland, Phil. Mag. 13, 1181 (1966); D. J. Stirland and D. S. Campbell, J. Vac. Sci. Technol. 3, 258 (1966).
14. J. L. Robins and T. N. Rhodin, Surf. Sci. 2, 346 (1964).
15. Ernst Bauer, Z. Krist. 110, 395 (1958).
16. B. K. Chakraverty and G. M. Pound, Proceedings of the International Symposium on Condensation and Evaporation of Solids (1962).
17. V. Halpern, Phys. Letters 32A, 2 (1970).
18. V. Halpern, J. Appl. Phys. 40, 4627 (1969).
19. P. W. Palmberg, T. N. Rhodin, and C. J. Todd, Proceedings of the Fourth International Vacuum Congress (1968).
20. R. Ueda and T. Inuzuka, J. Cryst. Growth 3,4, 191 (1968).

21. E. Grünbaum and J. W. Matthews, Phys. Stat. Solidi 9, 731 (1965).

22. H. Bethge, J. Vac. Sci. Technol. 6, 460 (1969).

23. H. Sato and S. Shinozaki, J. Appl. Phys. 41, 3165 (1970).

24. K. L. Chopra, Thin Film Phenomena (McGraw-Hill, 1969), p. 226.

25. H. Poppa, K. Heinemann, and A. Elliot, J. Vac. Sci. Technol. 8, 471 (1971).

26. C.A.O. Henning and J. S. Vermaak, Appl. Phys. Letters 15, 3 (1969).

27. M. Harsdorff, R. Adam, and H. Schmeisser, Kristall. und Technik 5, 279 (1970) and references cited therein.

28. E. Bauer, A. Green, K. Kunz, and H. Poppa, in Basic Problems in Thin Film Physics, ed. by R. Niedermayer and H. Mayer (Vandenhoeck and Ruprecht, Gottingen, 1966), p. 135.

29. R. W. Adam, Z. Naturforsch. 23a, 1526 (1968).

30. J. Matthews, Phil. Mag. 12, 1143 (1965).

31. T. Patrician and C. Wayman, Phys. Stat. Solidi (a) 6, 449 (1971).

32. C.A.O. Henning and J. S. Vermaak, Phil. Mag. 22, 281 (1970).

33. J. R. Roos and J. S. Vermaak, J. Cryst. Growth 13/14, 217 (1972).

34. E. Bauer and A. Green, Second Quarterly Report NASA Contract No. R-05-030-001, Aug. 1966.

35. H. Bethge and M. Krohn, Colloque Intern. CNRS (1965), No. 152, p. 391 and references given therein.

36. M. Hucher, A. Oberlin, and R. Hocart, Bull. Soc. Fr. Mineral Crist. 90, 320 (1967) and references given therein.

37. R. Lad, Surf. Sci. 12, 37 (1968).

38. A. Green, E. Bauer, and J. Dancy, J. Appl. Phys. 41, 4736 (1970).

39. R. Toth and L. Cicotte, Thin Solid Films 2, 111 (1968).

40. M. Birjega, F. Glodeanu, N. Popescu-Pogrion, I. Teodorescu, and V. Topa, Thin Solid Films 10, 307 (1972).

41. A. Sokol and V. Kosevich, Sov. Phys.--Crystallogr. 14, 438 (1969).

42. D. J. Stirland, Appl. Phys. Letters 8, 326 (1966).

43. A. Green, E. Bauer, and J. Dancy, Molecular Processes on Solid Surfaces (1969).

44. D. J. Stirland, Thin Solid Films 1, 447 (1967/68).

45. D. J. Stirland, Appl. Phys. Letters 15, 86 (1969).

46. P. W. Palmberg and T. N. Rhodin, J. Phys. Chem. Solids 29, 1917 (1968).

47. T. E. Gallon, I. G. Higginbotham, M. Prutton, and H. Tokutaka, Surf. Sci. 21, 224 (1970).

48. D. G. Lord, Thin Solid Films 7, R39 (1971).

49. T. E. Gallon, I. G. Higginbotham, M. Prutton, and H. Tokutaka, Thin Solid Films 2, 369 (1968).

50. R. A. Lad, private communication.

51. R. A. Lad and G. Fryburg (NASA TMX-52989), Physical Society Meeting, Cleveland, March 29-April 1, 1971.

52. T. Inuzuka and R. Ueda, Appl. Phys. Letters 13, 3 (1968); J. Phys. Soc. Japan 25, 1299 (1968); J. Cryst. Growth 3,4, 191 (1968); J. Cryst. Growth 9, 79 (1971).

53. G. Distler, V. N. Lebedeva, and V. V. Moskvin, Sov. Phys.--Crystallogr. 14, 559 (1970).

54. F. Forssell, B. Persson, and L. Yström, Physica Scripta 2, 303 (1970).

55. A. Scott, W. Smith, and M. Thompson, J. Phys. Chem. 57, 757 (1953).

56. K. Mihama and M. Tanaka, J. Cryst. Growth 2, 51 (1968).

57. E. Krimmel and A. Gordon, Z. Angew. Phys. 22, 1 (1966).

58. E. Krimmel and W. Kurtz, Grenoble Electron Microscopy Conference (1970) p. 441.

59. C. Layton and D. Campbell, J. Mat. Sci. 1, 367 (1966).

60. K. L. Chopra, Appl. Phys. Letters 7, 140 (1965).

61. K. L. Chopra, J. Appl. Phys. 37, 2249 (1966).

62. Y. Murayama, K. Kashiwagi, and M. Matsumoto, J. Phys. Soc. Japan 31, 303 (1971).

63. Y. Murayama, 1972 International Conference on Thin Films, 15-19 May, Venice, Italy.

64. G. I. Distler, J. Cryst. Growth 9, 76 (1971) and references therein.

65. G. I. Distler, S. A. Kobzareva, and Y. M. Gerasimov, Proceedings Second Colloq. Thin Films (1967), p. 81, and references therein.

66. G. I. Distler and E. I. Tokmakova, Sov. Phys.--Crystallogr. 16, 171 (1971).

67. Á. Barna, P. B. Barna, and J. F. Pócza, Thin Solid Films 4, R32 (1969).

68. K. Chopra, J. Appl. Phys. 40, 906 (1969).

69. K. Chopra, Surf. Sci. 20, 201 (1970).

70. K. Hayek and U. Schwabe, Surf. Sci. 19, 329 (1970).

71. K. Hayek and U. Schwabe, Grenoble Electron Microscopy Conference (1970) p. 327.

72. C. Henning, Nature 227, 1129 (1970).

TABLE I. Summary: Influence of Defects and Impurities on Nucleation.

0-dimension	Number	Orientation	Example for NaCl
vacancies	yes	no	electron preirradiation
F-Centers	no	no	x-ray irradiation
adsorbed atoms	yes	yes	electron irradiation
1-dimension			
steps	yes	no	vacuum cleaved
grain boundaries	yes	no	
slip plane intersections	yes	no	
2-dimension			
precipitates	no	no	vac-cleaved, Ca-doped
colloids	yes	yes	Ag-doped; additive color
adsorbed layers	no	no	H_2O exposed

FIGURE CAPTIONS

Fig. 1. Selected decoration structures on vac-cleaved NaCl. (Au/NaCl, $P = 2 \times 10^{-8}$ Torr, T = 275°C, r ≃ 0.35 Å/sec, 5 Å exposure.)

Fig. 2. Classification of defects.

Fig. 3. Decoration structure of (A) air- and (B) vac-cleaved NaCl. (Au/NaCl, $P = 1 \times 10^{-8}$ Torr, T = 270°C, r ≃ 0.1 Å/sec, 4 Å exposure.)

Fig. 4. Decoration of unirradiated (A) and irradiated (B) vac-cleaved NaCl. (Au/NaCl, $P = 1 \times 10^{-9}$ Torr, T = 200°C, r ≃ 0.32 Å/sec, 12 Å exposure.)

Fig. 5. Particle orientation determination by "Bragg Reflex Image" technique using "selected zone dark field"; (A) bright field and (B) dark field. (Au/NaCl, vac-cleaved, $P = 2 \times 10^{-8}$ Torr, T = 275°C, r ≃ 0.35 Å/sec, 5 Å exposure.)

Fig. 6. Decoration structure of (A) air- and (B) vac-cleaved NaCl. (Au/NaCl, $P = 1 \times 10^{-8}$ Torr, T = 270°C, r ≃ 0.1 Å/sec, 4 Å exposure.)

Fig. 7. Typical decoration structure of (A) air- and (B) vac-cleaved NaCl. (Same deposition as in Fig. 6) Note predominant epitaxial orientation.

Fig. 8. Au/NaCl at slightly higher rate than in Fig. 7; (A) air- and (B) vac-cleaved. ($P = 1 \times 10^{-8}$ Torr, T = 270°C, r ≃ 0.3 Å/sec, 4 Å exposure.) Note MTP diffraction pattern.

Fig. 9. Au/NaCl deposited at low rate with 19 Å exposure; (A) air- and (B) vac-cleaved. ($P = 1 \times 10^{-8}$ Torr, T = 280°C, r ≃ 0.1 Å/sec.)

Fig. 10. Au/NaCl deposited at low rate with 200 Å exposure; (A) air- and (B) vac-cleaved. ($P = 5 \times 10^{-8}$ Torr, T = 275°C, r ≃ 0.1 Å/sec.)

Fig. 11. Au/NaCl continuous film; (A,B) air- and (C,D) vac-cleaved. ($P = 2 \times 10^{-8}$ Torr, T = 270°C.)

Fig. 12. Au/NaCl with and without Cl_2 exposures (T = 150°C, r ≃ 0.2 Å/sec, 100 Å Au exposure. (A) TEM and TED, P = 3 x 10^{-8} Torr (no Cl_2 leak); (B) corresponding RHEED; (C) TEM and TED, P = 5 x 10^{-7} Torr (controlled leak); (D) corresponding RHEED.

Fig. 13. Au film grown on vac-cleaved NaCl at room temperature. (P ≃ 5 x 10^{-7} Torr (controlled Cl_2 leak) r ≃ 0.1 Å/sec, 14 Å Au exposure.)

Fig. 14. Au grown on undoped (A,B) and 0.2 mole % Ca-doped NaCl (C,D), vac-cleaved. (P = 1 x 10^{-8} Torr, T = 340°C, r ≃ 0.5 Å/sec, ~ 10 Å exposure.)

Fig. 15. Au grown on 0.2 mole % Ca-doped NaCl; (A,B) air- and (C,D) vac-cleaved. (P = 1 x 10^{-8} Torr, T = 340°C, r ≃ 0.5 Å/sec, ~ 10 Å exposure.)

Fig. 16. Au film deposited on unirradiated (A,B), preirradiated (C,D) and simultaneously irradiated (E,F) vac-cleaved NaCl. (P = 1 x 10^{-4} Torr, T = 200°C, r ≃ 0.3 Å/sec, 10 Å exposure.)

Fig. 17. (A-D) Model for growth of epitaxial Au nuclei on NaCl surface with a Cl^- vacancy (after Rhodin et al.), (E) 45° orientation of 5-atom nucleus (after Stirland).

Fig. 18. In situ RHEED patterns showing the development of (100) $NaAu_2$ by electron irradiation of a thin Au film at 330°C. (A) (100) Au with NaCl streak pattern, (B) first $NaAu_2$ spots, (C) intense $NaAu_2$ pattern ⟨110⟩ azimuth, (D) ⟨100⟩ azimuth $NaAu_2$ pattern.

Fig. 19. Au deposited simultaneously, with (A,B) and without (C,D), -2.5 kV screen in vapor path. (P = 4 x 10^{-9} Torr, T = 250°C, r ≃ 0.1 Å/sec.)

Fig. 20. PbS deposited on NaCl with intermediate layers of SiO. (A-C) are 20, 40 and 80 Å, respectively, of SiO; (D-F) are 40 Å of PbS on each of the SiO layers; (G-I) are TED patterns of the composite PbS-SiO films. ($P = 5 \times 10^{-6}$ Torr, T = 300°C, r ≃ 2.5 Å/sec, 40 Å PbS exposure.)

Fig. 21. PbS deposited on (A) air- and (B) vac-cleaved NaCl with 80 Å SiO intermediate layer. ($P = 5 \times 10^{-6}$ Torr, T = 325°C, r ≃ 3.5 Å/sec, 80 Å PbS exposure.)

SELECTED DECORATION PATTERNS Au ON VAC–CLEAVED NaCl

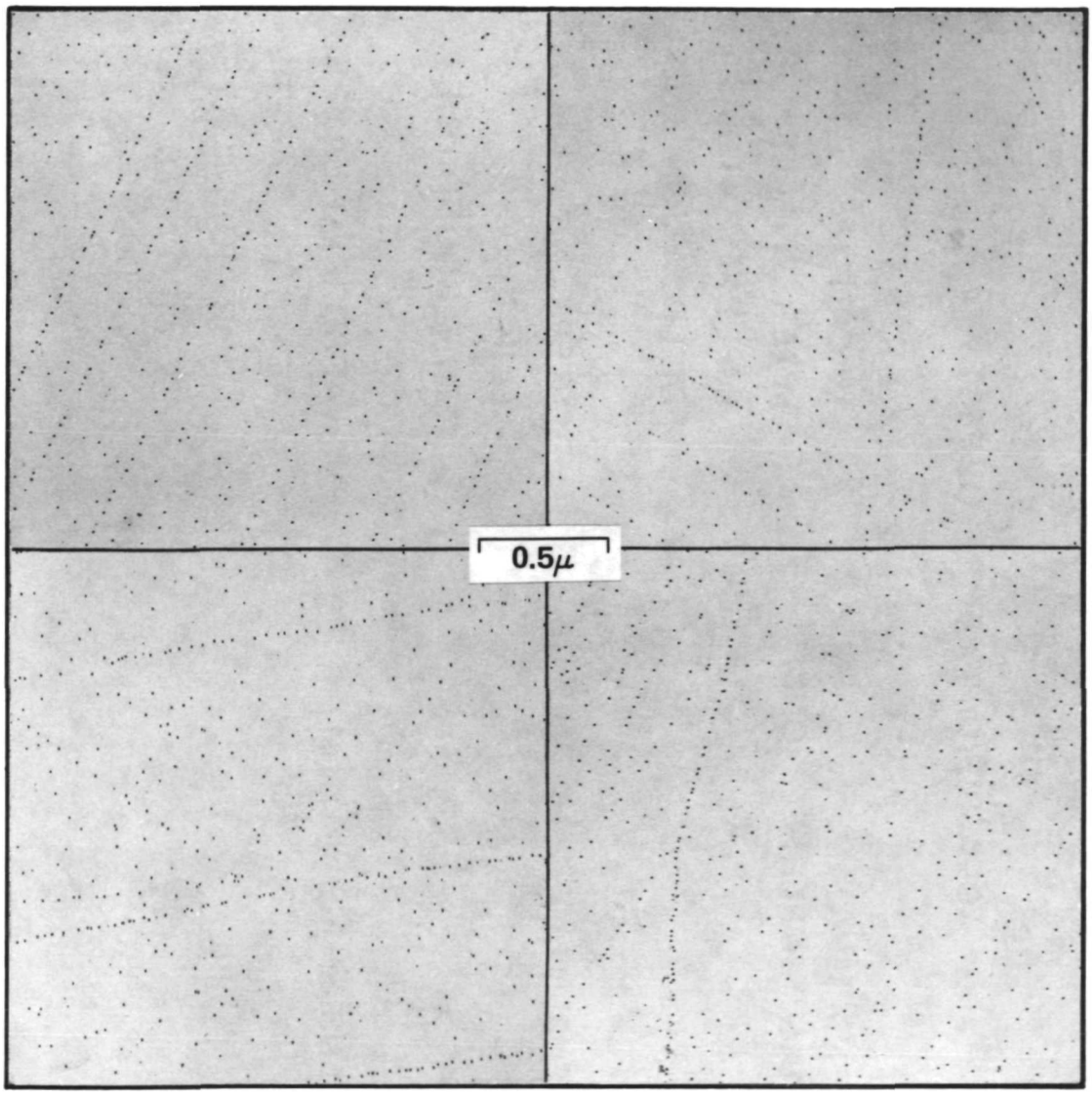

T=275°C, r = 0.3Å /sec, 5Å EXPOSURE

Figure 1.

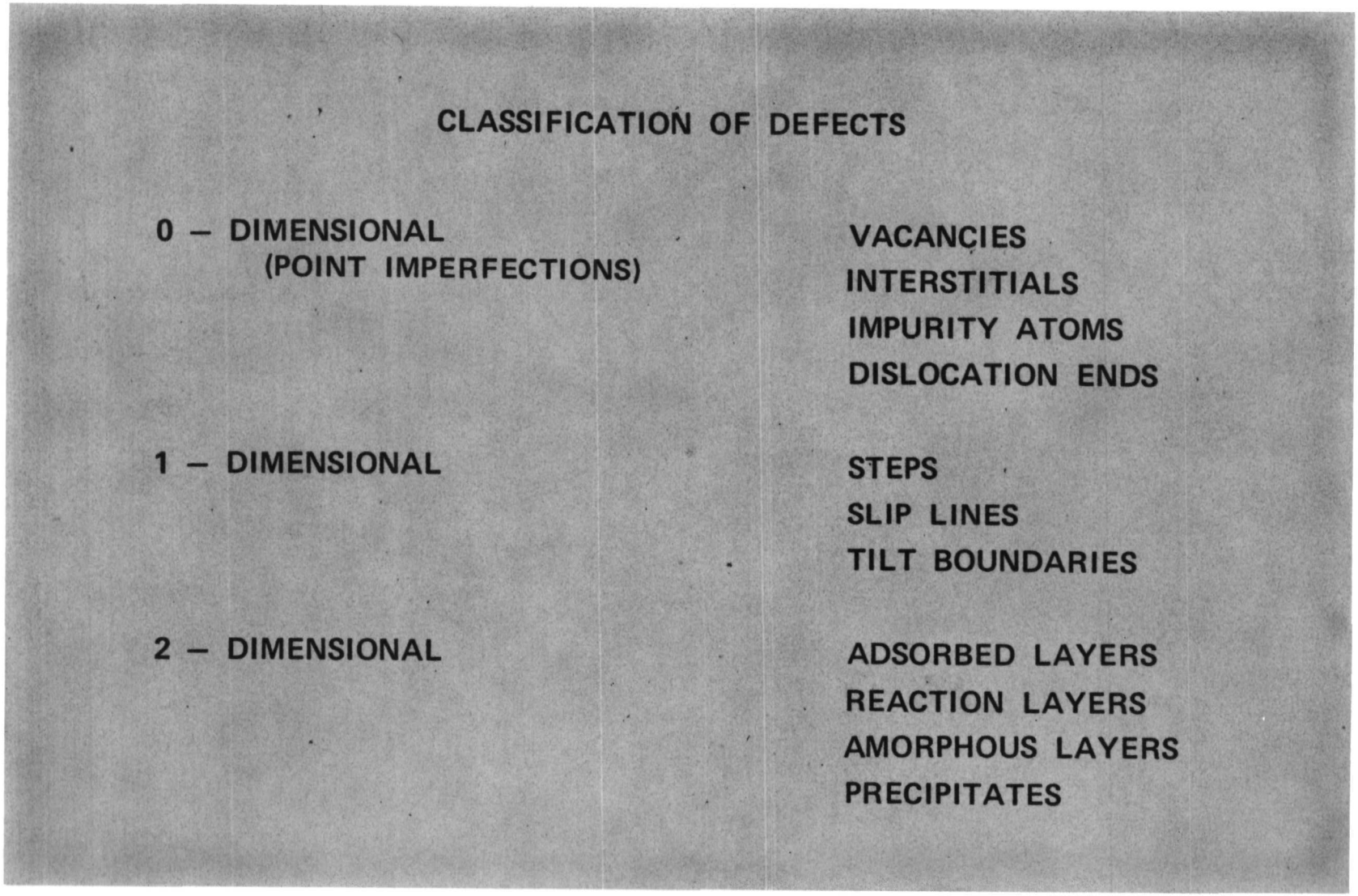
CLASSIFICATION OF DEFECTS
0 – DIMENSIONAL
(POINT IMPERFECTIONS)
VACANCIES
INTERSTITIALS
IMPURITY ATOMS
DISLOCATION ENDS
1 – DIMENSIONAL
STEPS
SLIP LINES
TILT BOUNDARIES
2 – DIMENSIONAL
ADSORBED LAYERS
REACTION LAYERS
AMORPHOUS LAYERS
PRECIPITATES

Figure 2.

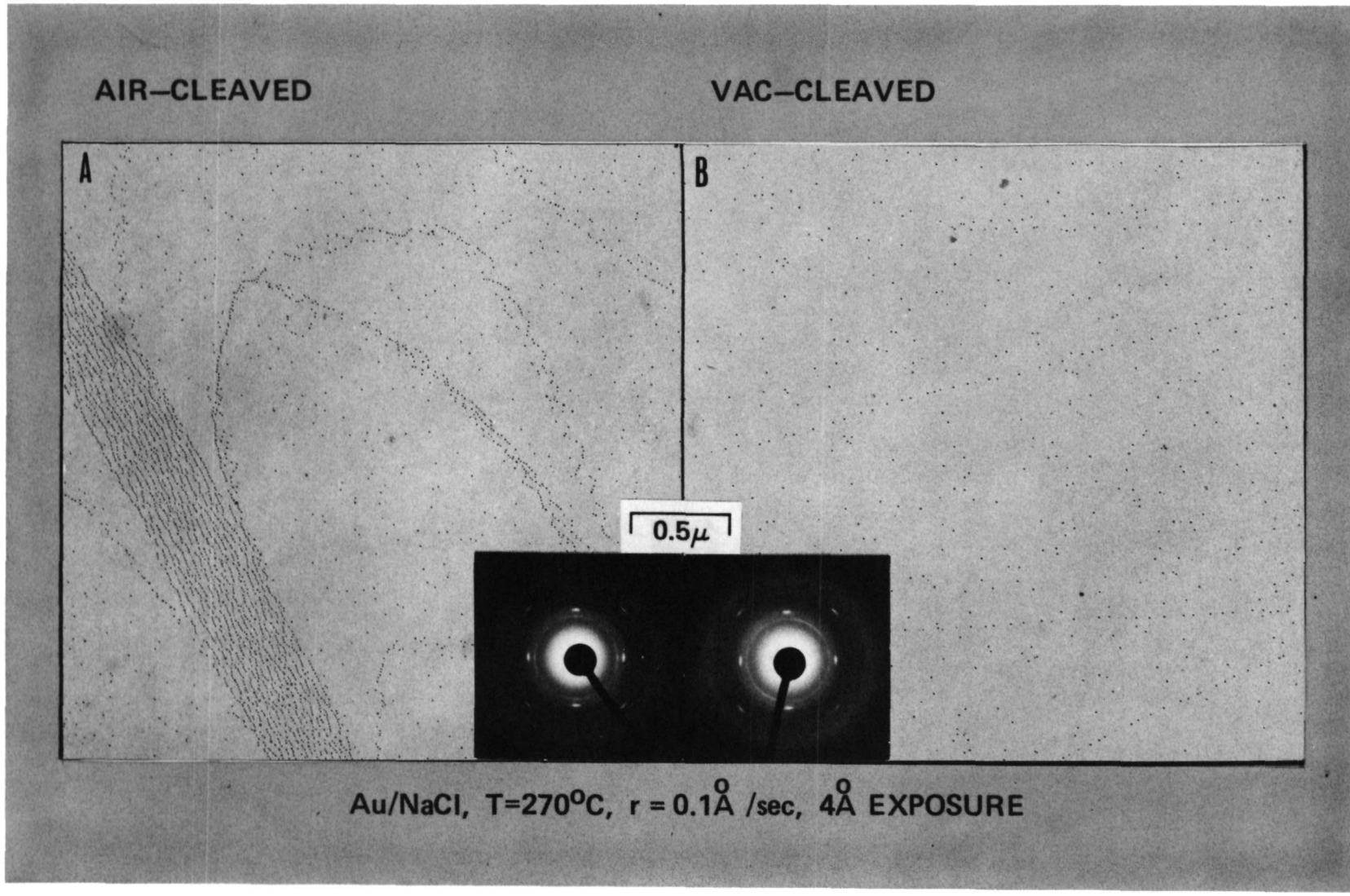
AIR–CLEAVED
VAC–CLEAVED
A
B
0.5μ
Au/NaCl, T=270°C, r = 0.1Å /sec, 4Å EXPOSURE

Figure 3.

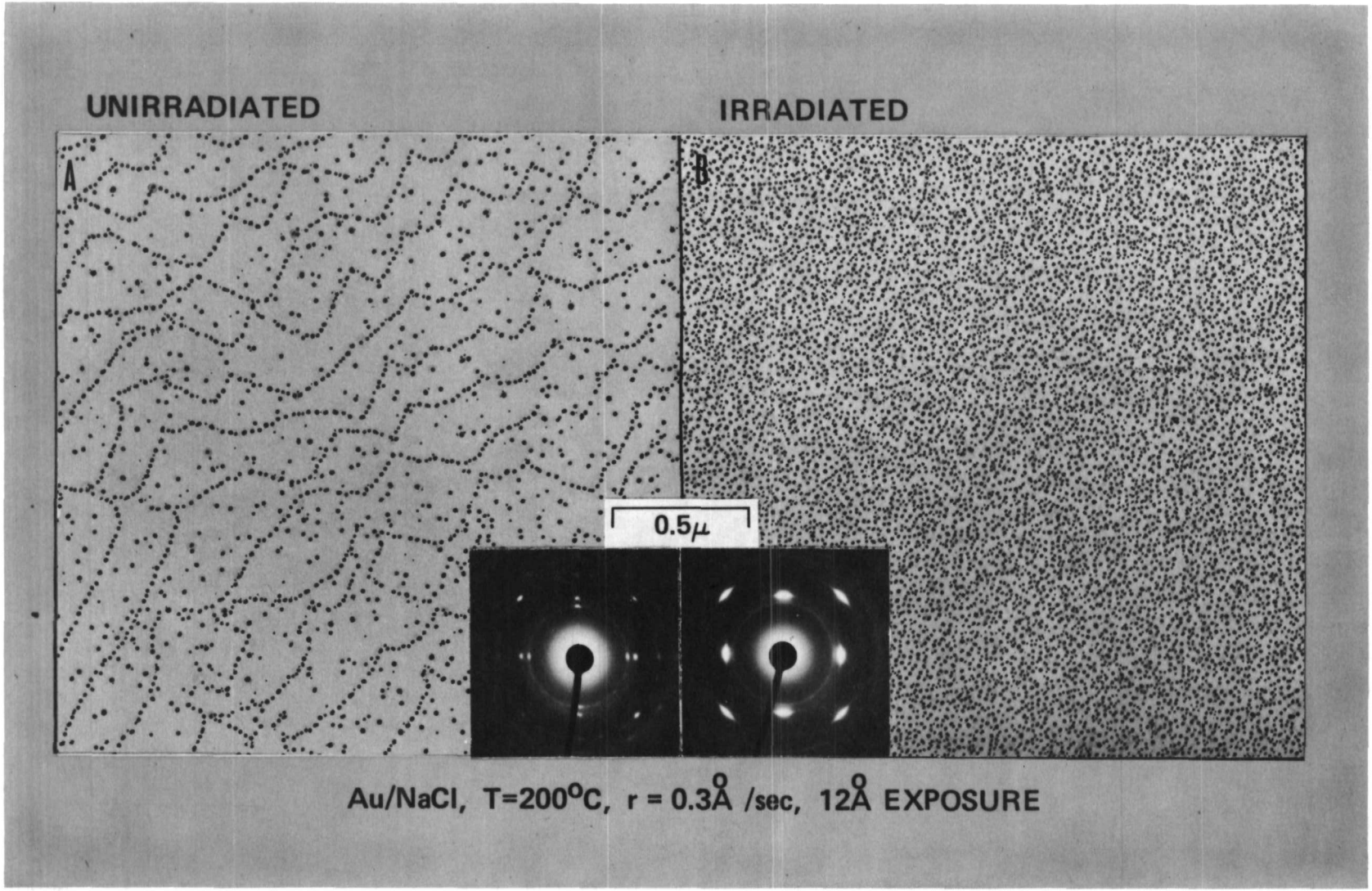
UNIRRADIATED
IRRADIATED
A
B
0.5μ
Au/NaCl, T=200°C, r = 0.3Å /sec, 12Å EXPOSURE

Figure 4.

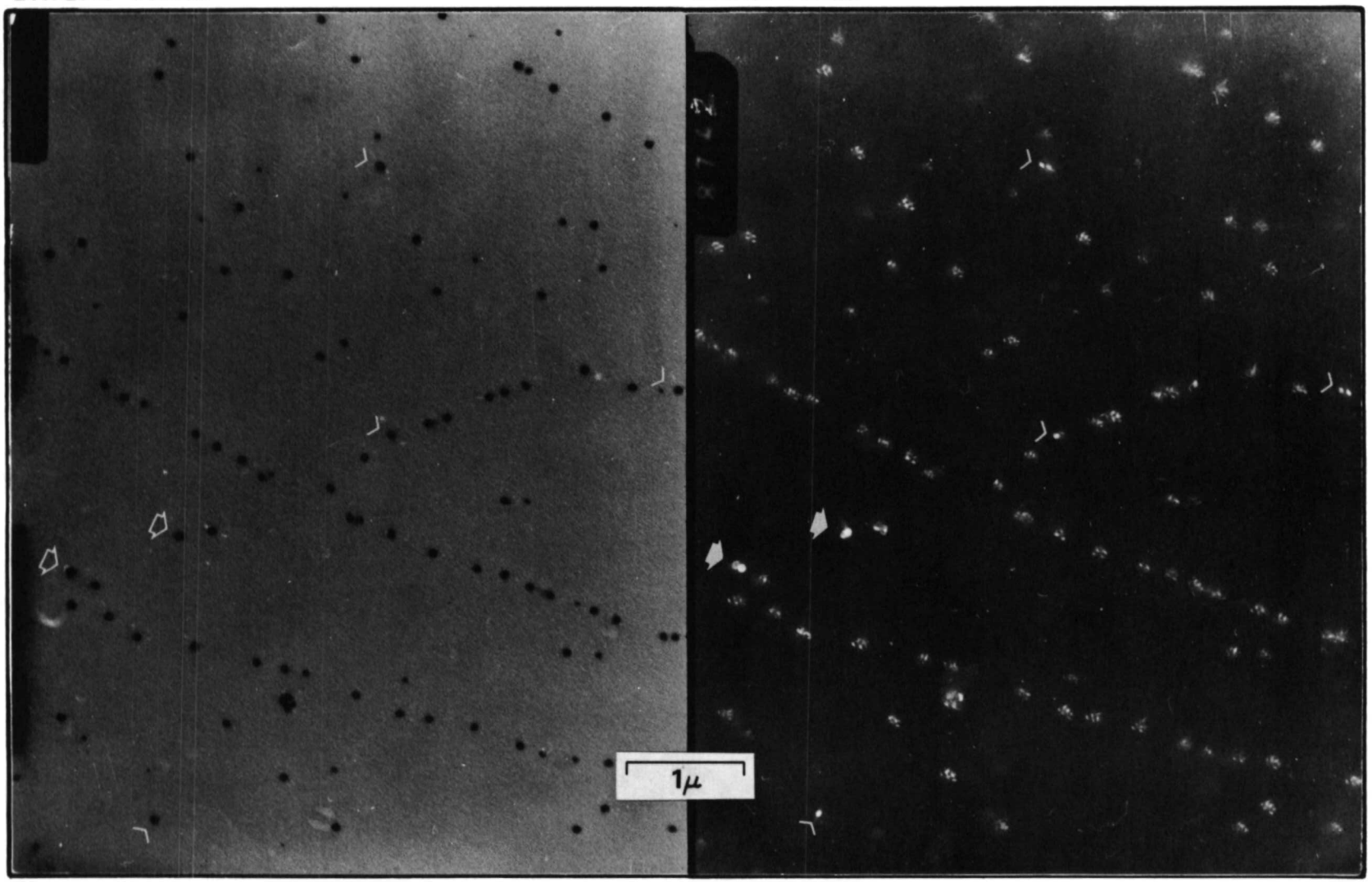

Au/NaCl, T=275°C, r = 0.3Å /sec, 5Å EXPOSURE

Figure 5.

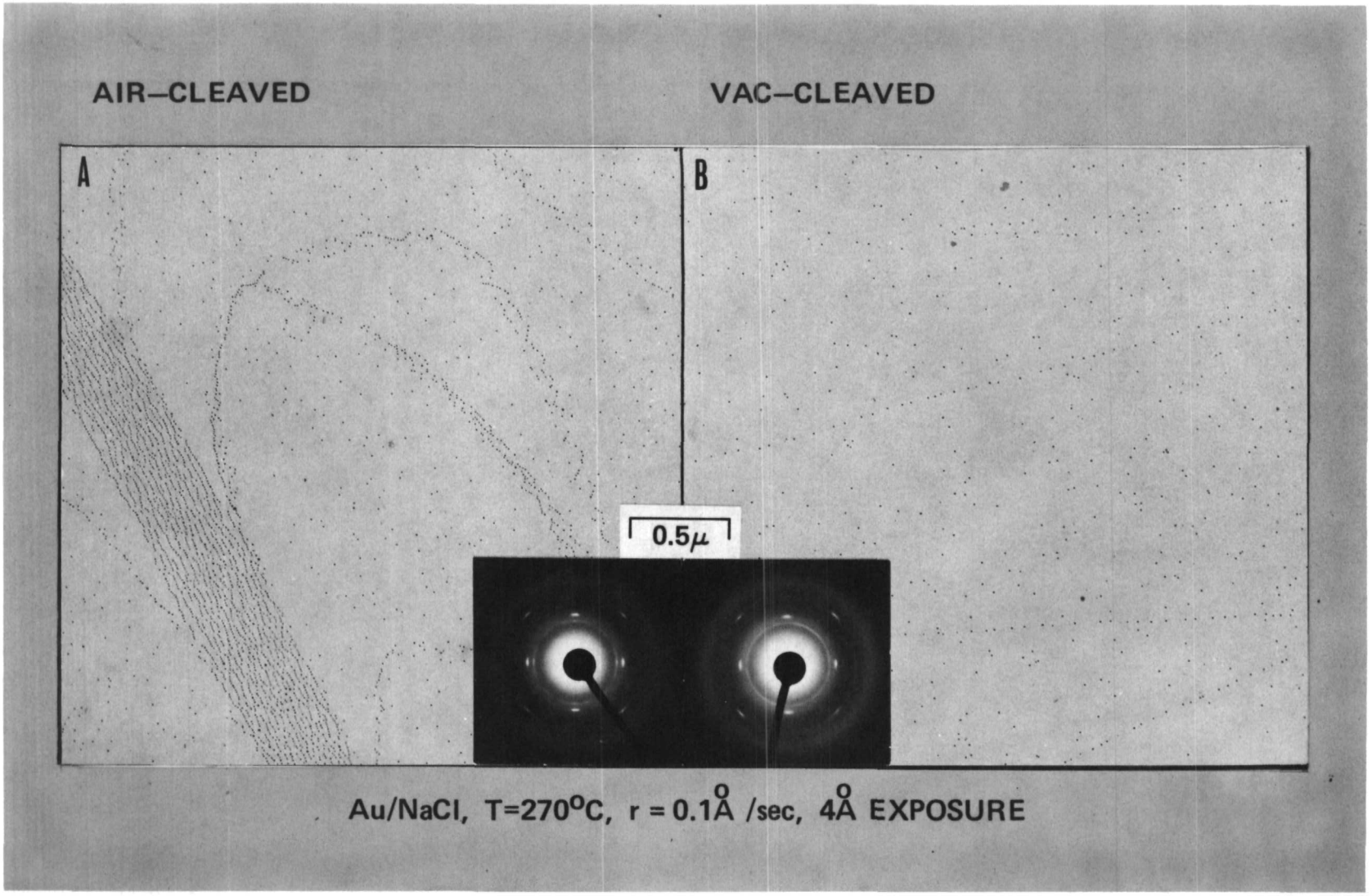
AIR–CLEAVED
VAC–CLEAVED
A
B
0.5μ
Au/NaCl, T=270°C, r = 0.1Å /sec, 4Å EXPOSURE

Figure 6.

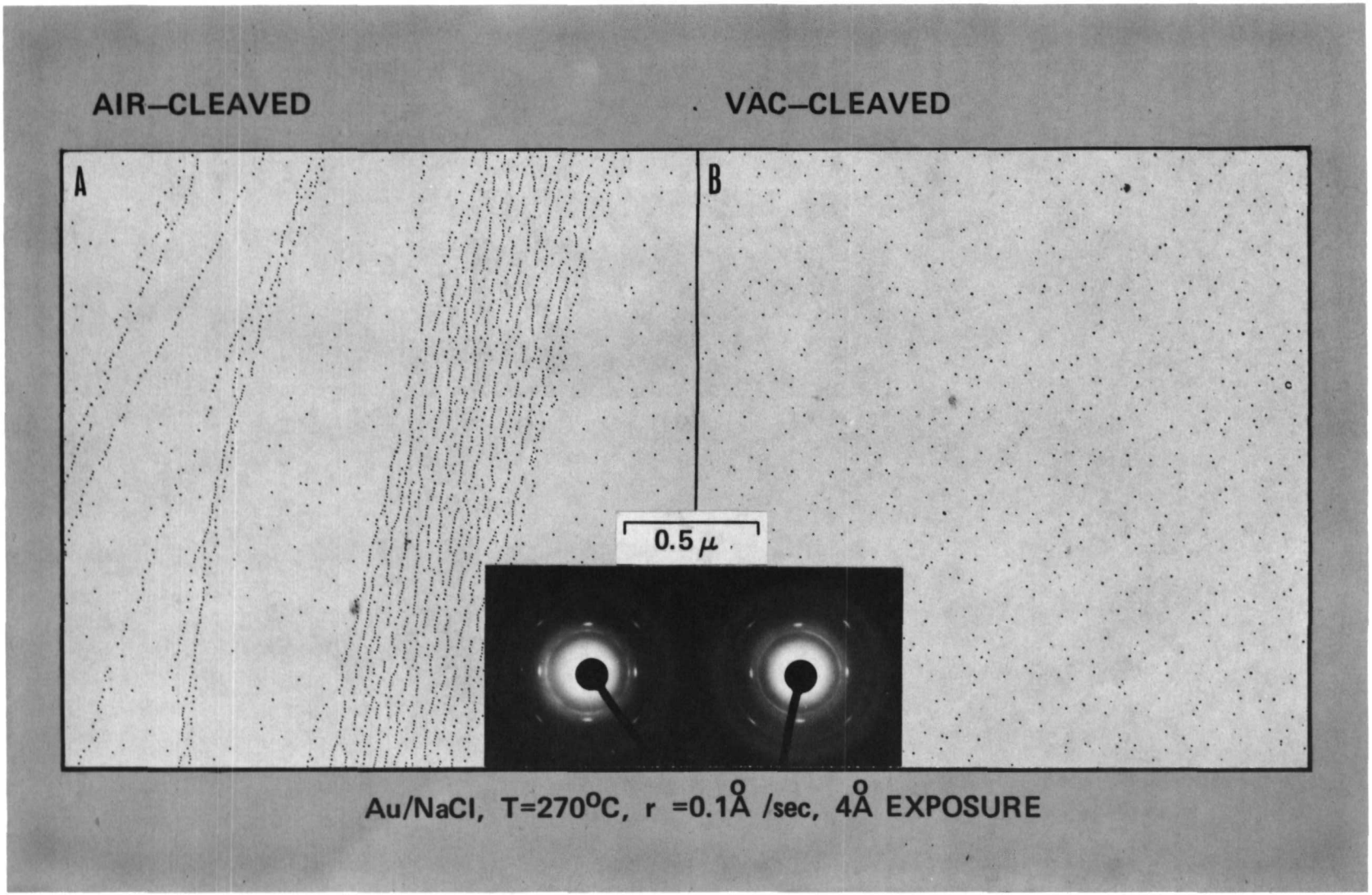
AIR–CLEAVED
VAC–CLEAVED
A
B
0.5 μ
Au/NaCl, T=270°C, r =0.1Å /sec, 4Å EXPOSURE

Figure 7.

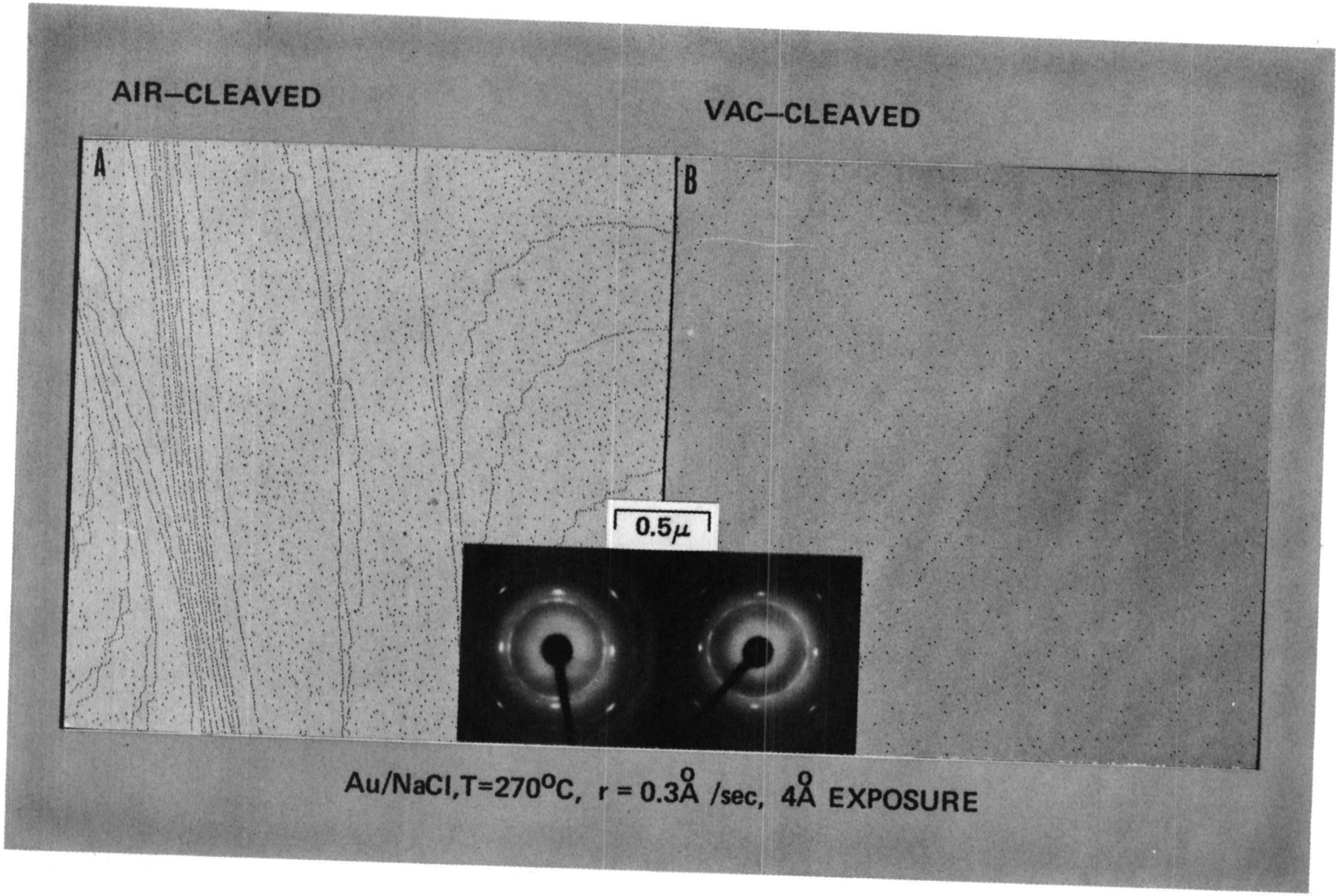
AIR–CLEAVED
VAC–CLEAVED
A
B
0.5μ
Au/NaCl,T=270°C, r = 0.3Å /sec, 4Å EXPOSURE

Figure 8.

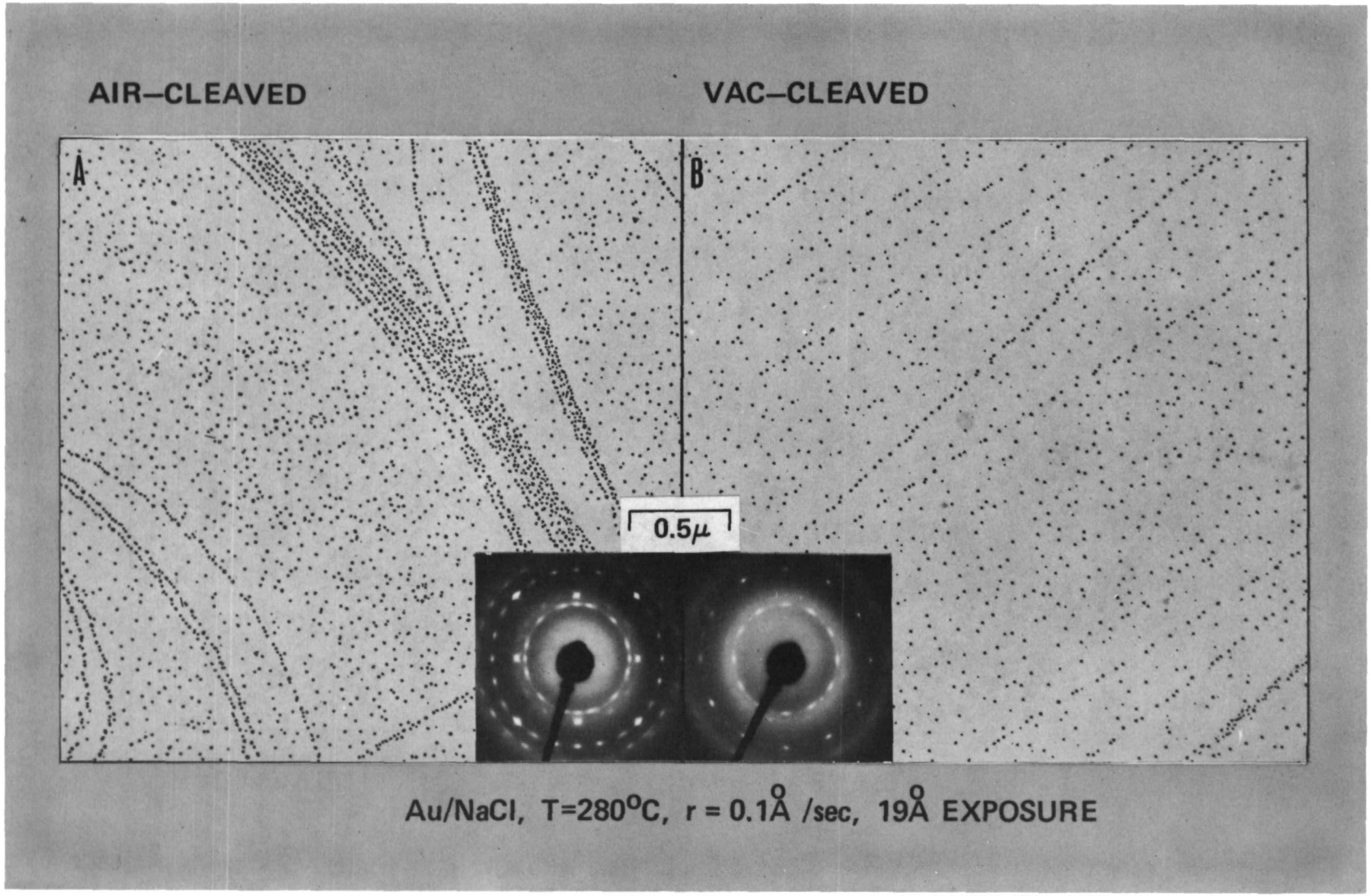
AIR–CLEAVED
VAC–CLEAVED
A
B
0.5μ
Au/NaCl, T=280°C, r = 0.1Å /sec, 19Å EXPOSURE

Figure 9.

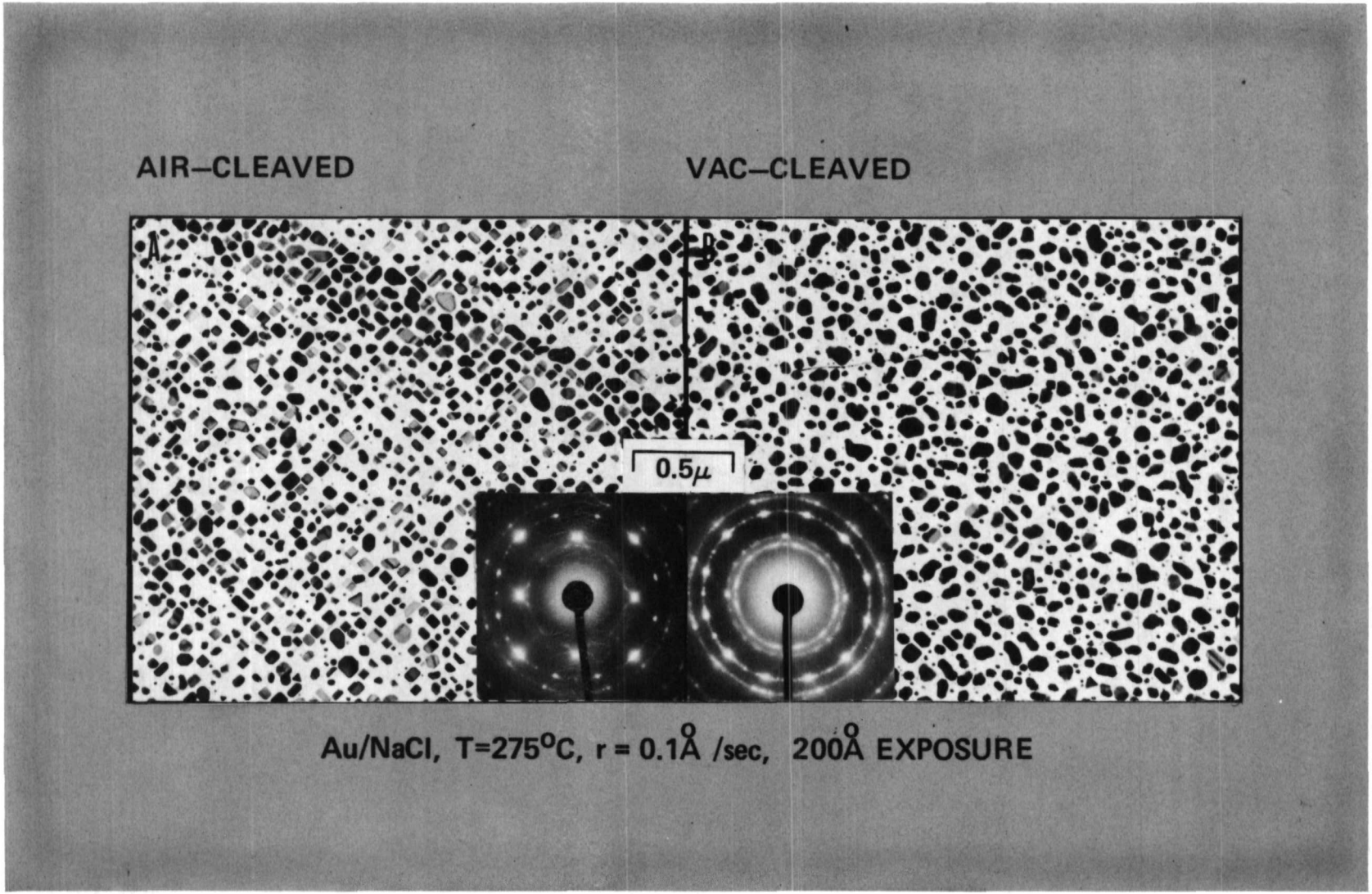
AIR–CLEAVED
VAC–CLEAVED
A
B
0.5μ
Au/NaCl, T=275°C, r = 0.1Å /sec, 200Å EXPOSURE

Figure 10.

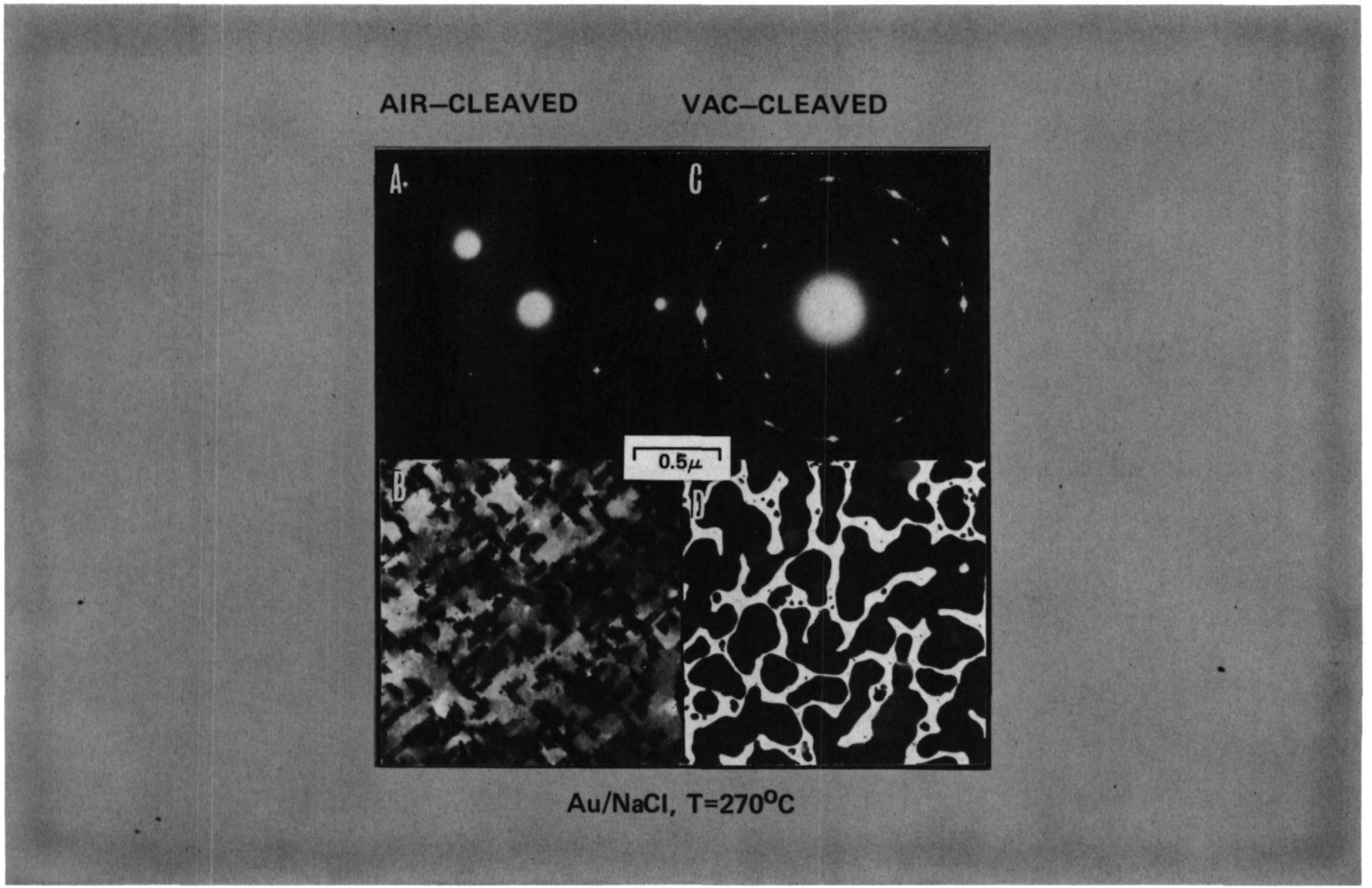

Figure 11.

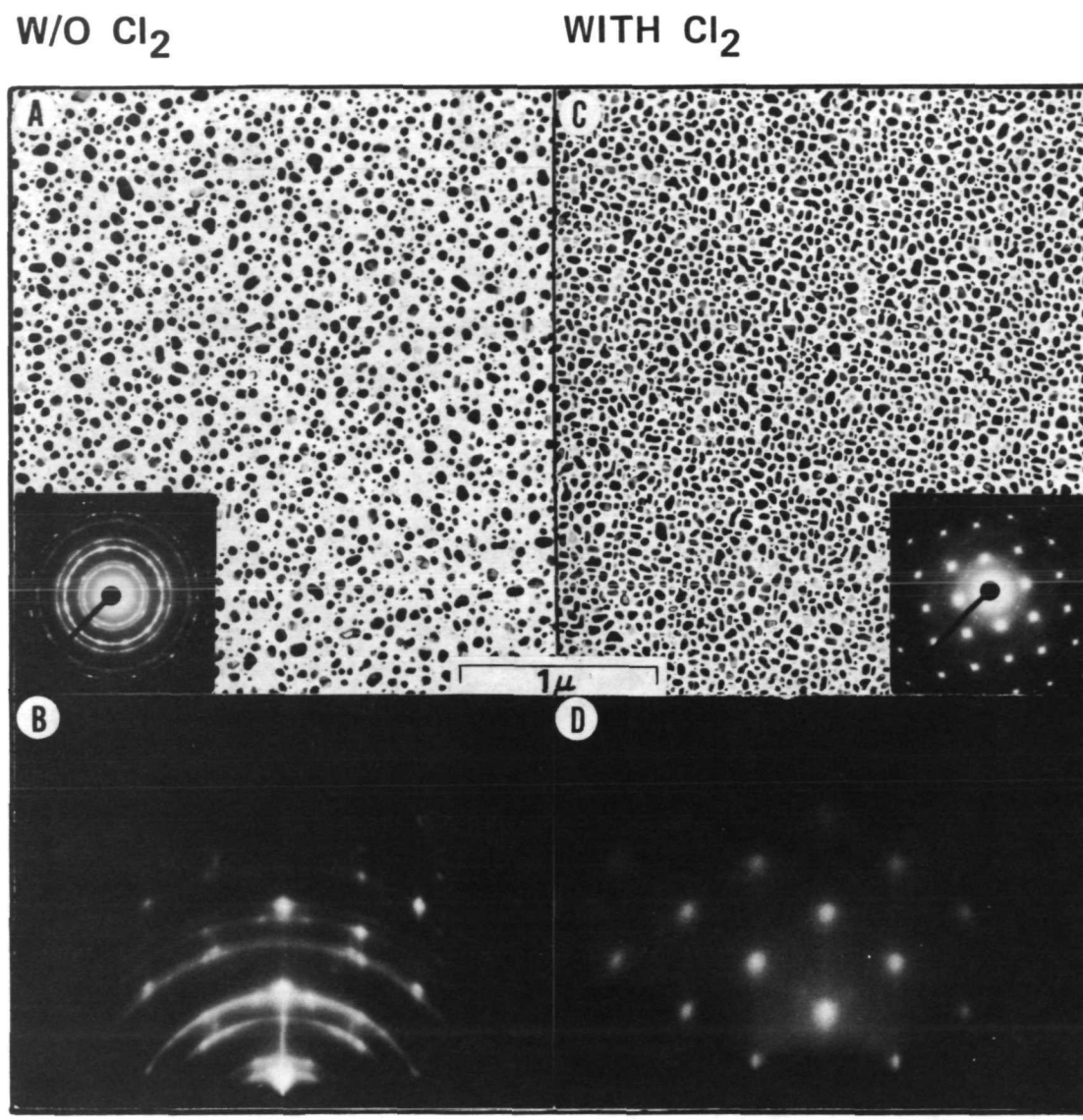

Figure 12.

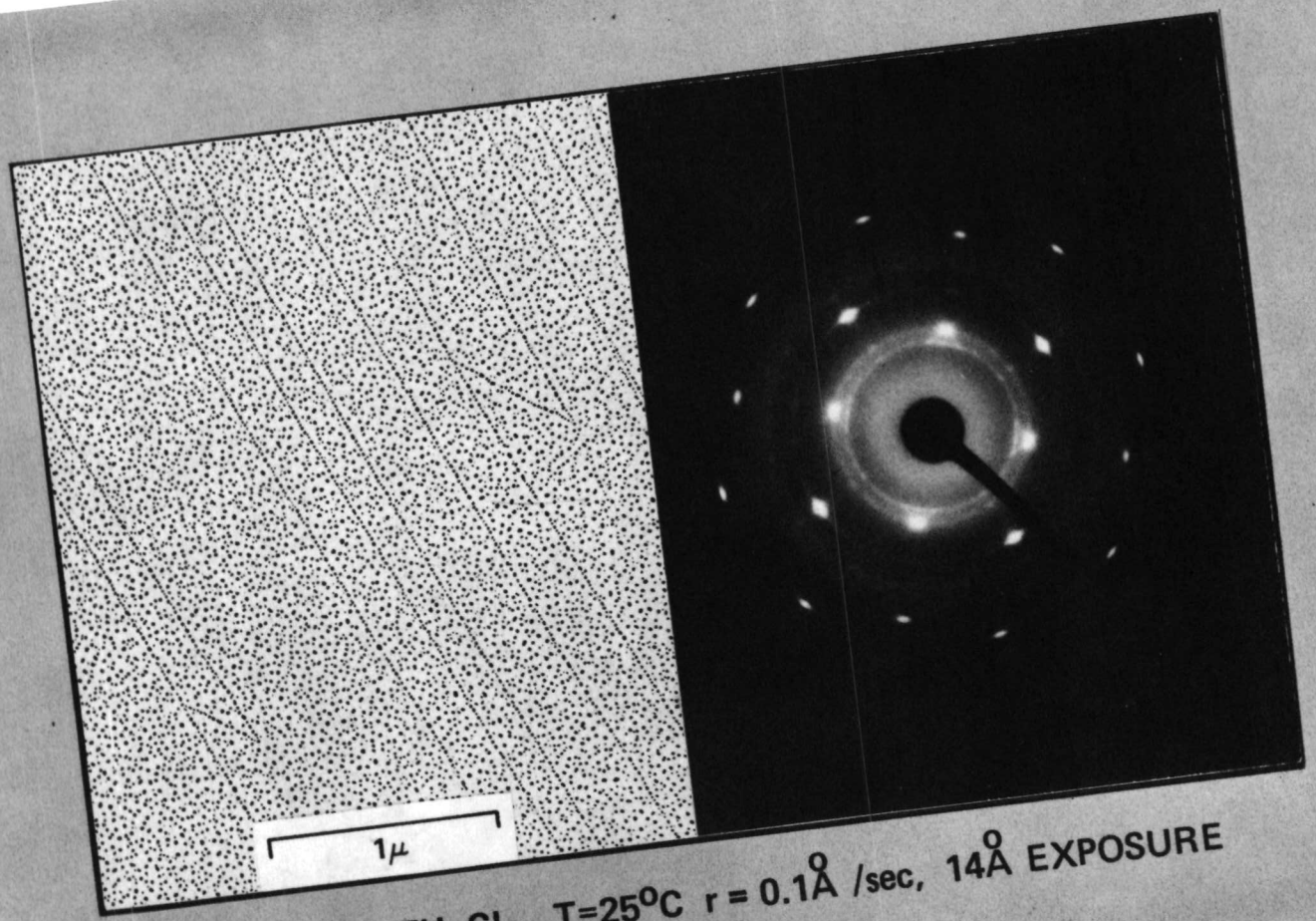

Figure 13.

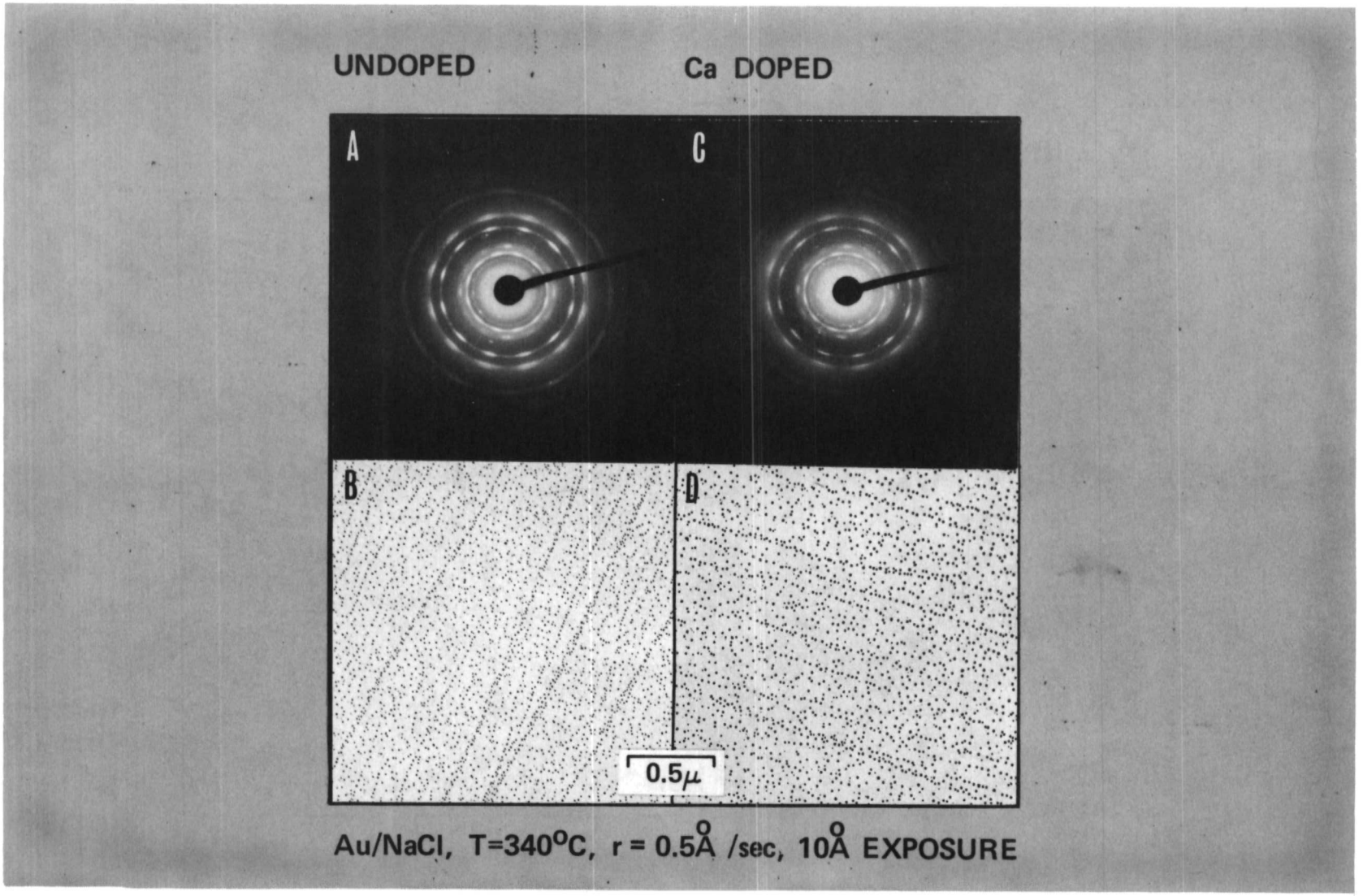
UNDOPED
Ca DOPED
A
C
B
D
0.5μ
Au/NaCl, T=340°C, r = 0.5Å /sec, 10Å EXPOSURE

Figure 14.

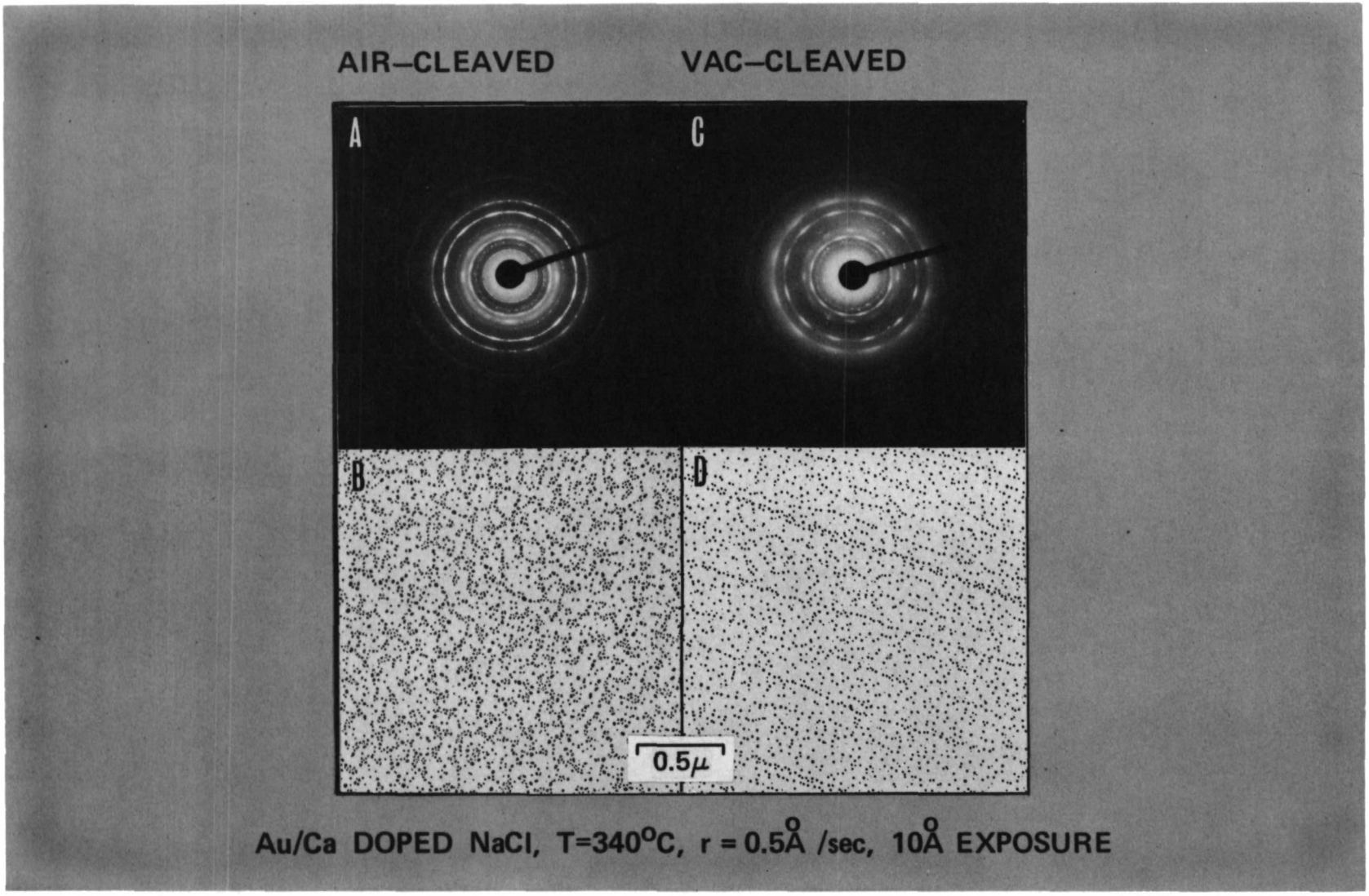
AIR–CLEAVED
VAC–CLEAVED
A
C
B
D
0.5μ
Au/Ca DOPED NaCl, T=340°C, r = 0.5Å /sec, 10Å EXPOSURE

Figure 15.

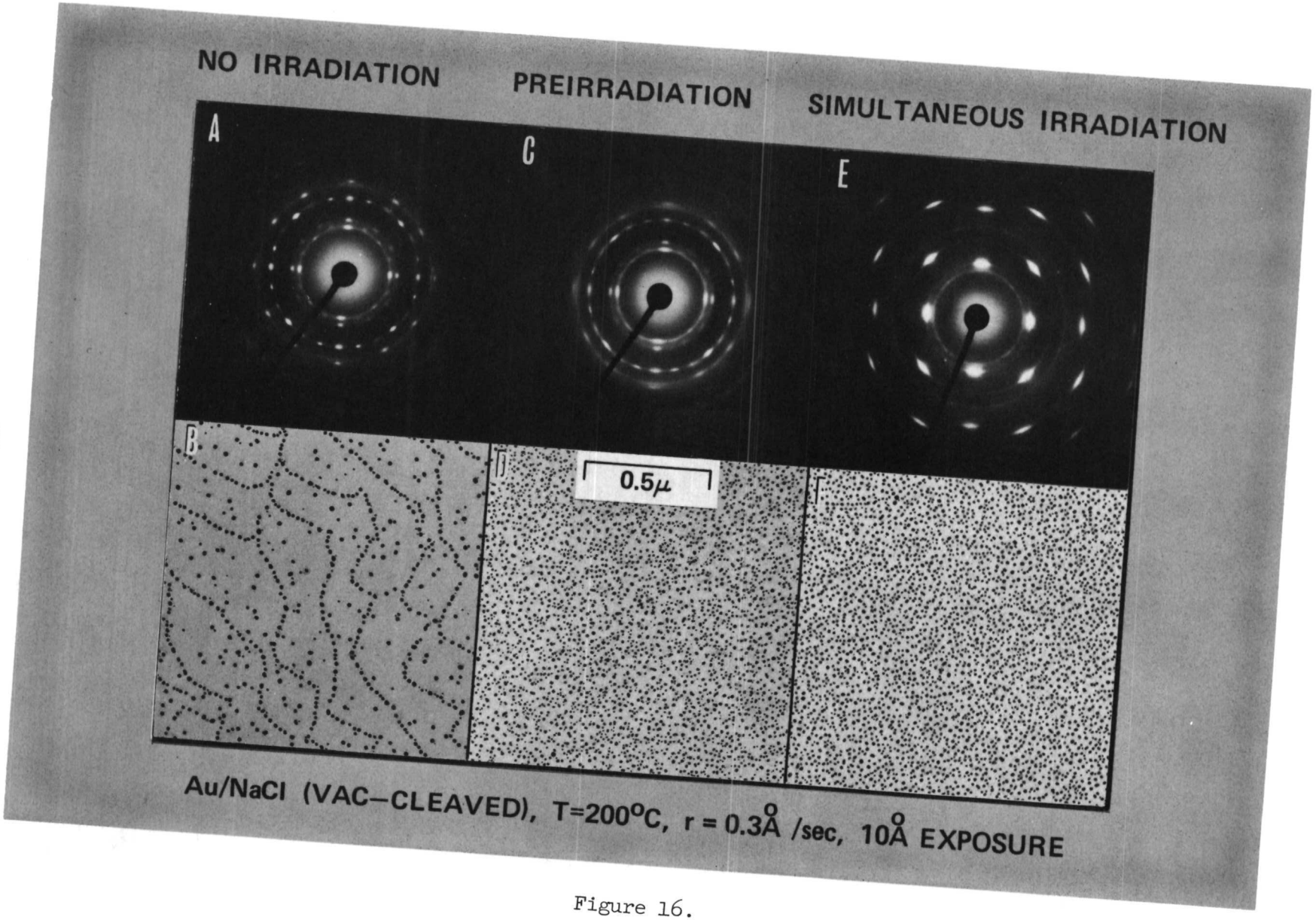
NO IRRADIATION
PREIRRADIATION
SIMULTANEOUS IRRADIATION
A
C
E
B
D
F
0.5μ
Au/NaCl (VAC–CLEAVED), T=200°C, r = 0.3Å /sec, 10Å EXPOSURE

Figure 16.

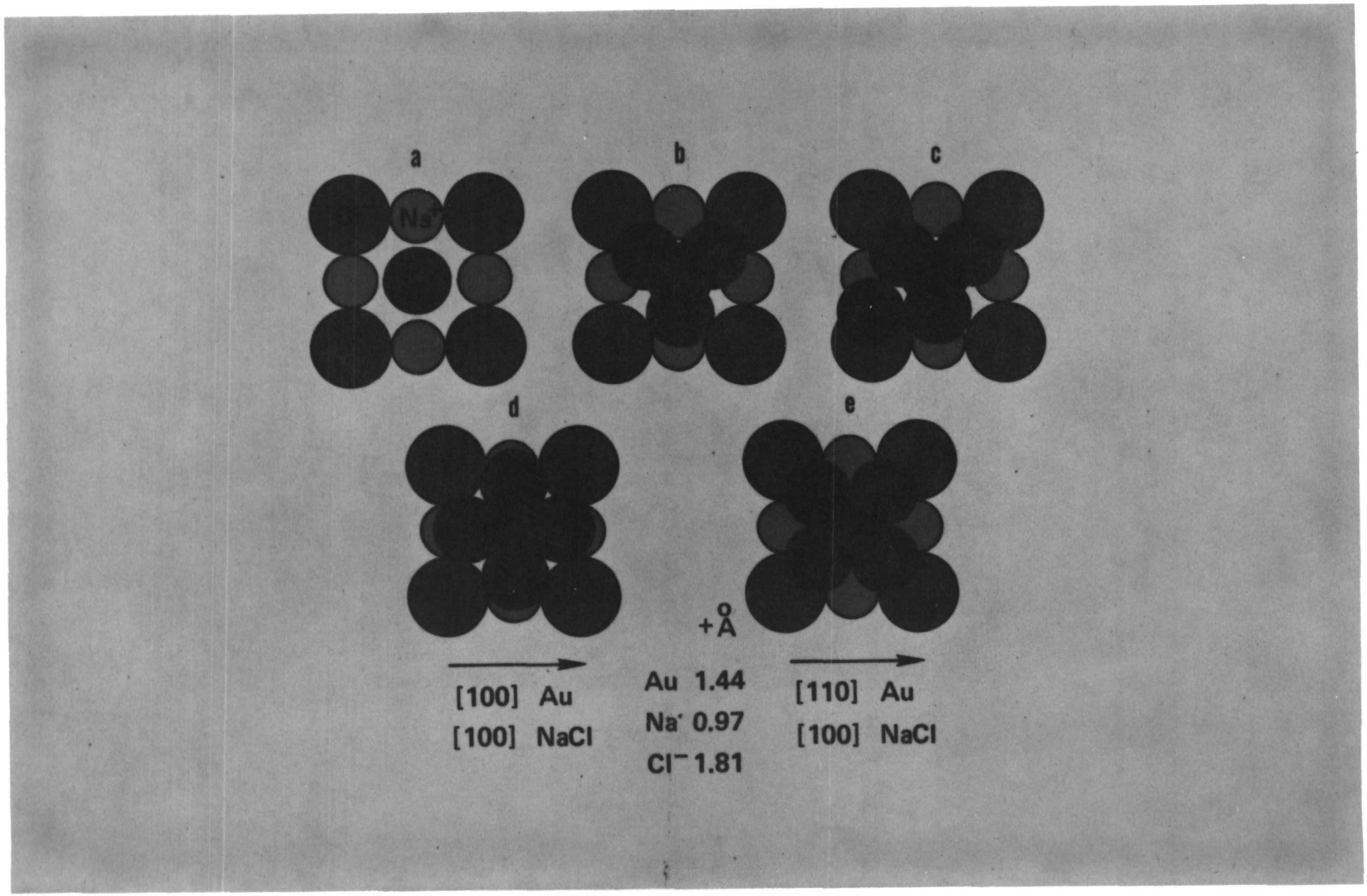

Figure 17.

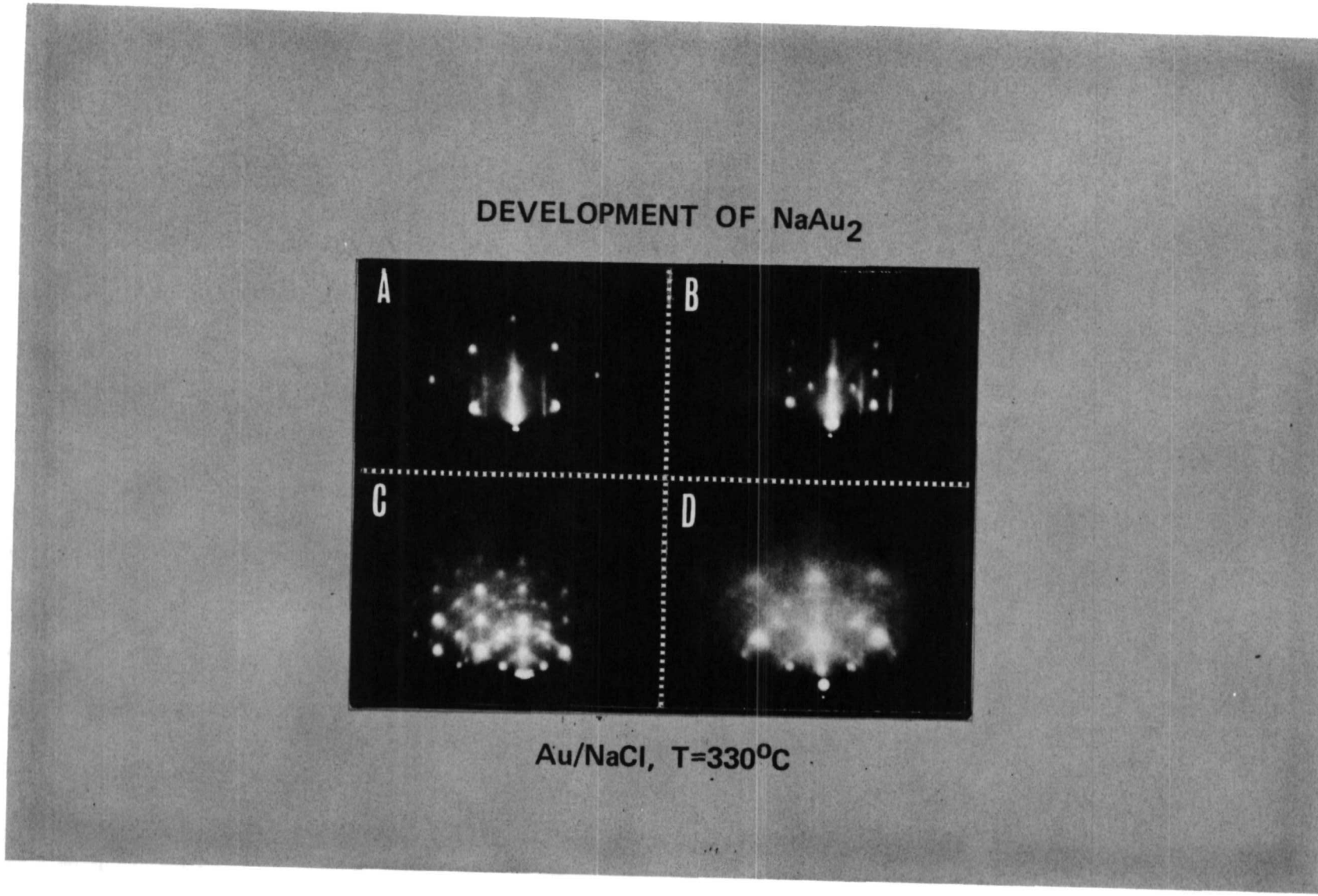

Figure 18.

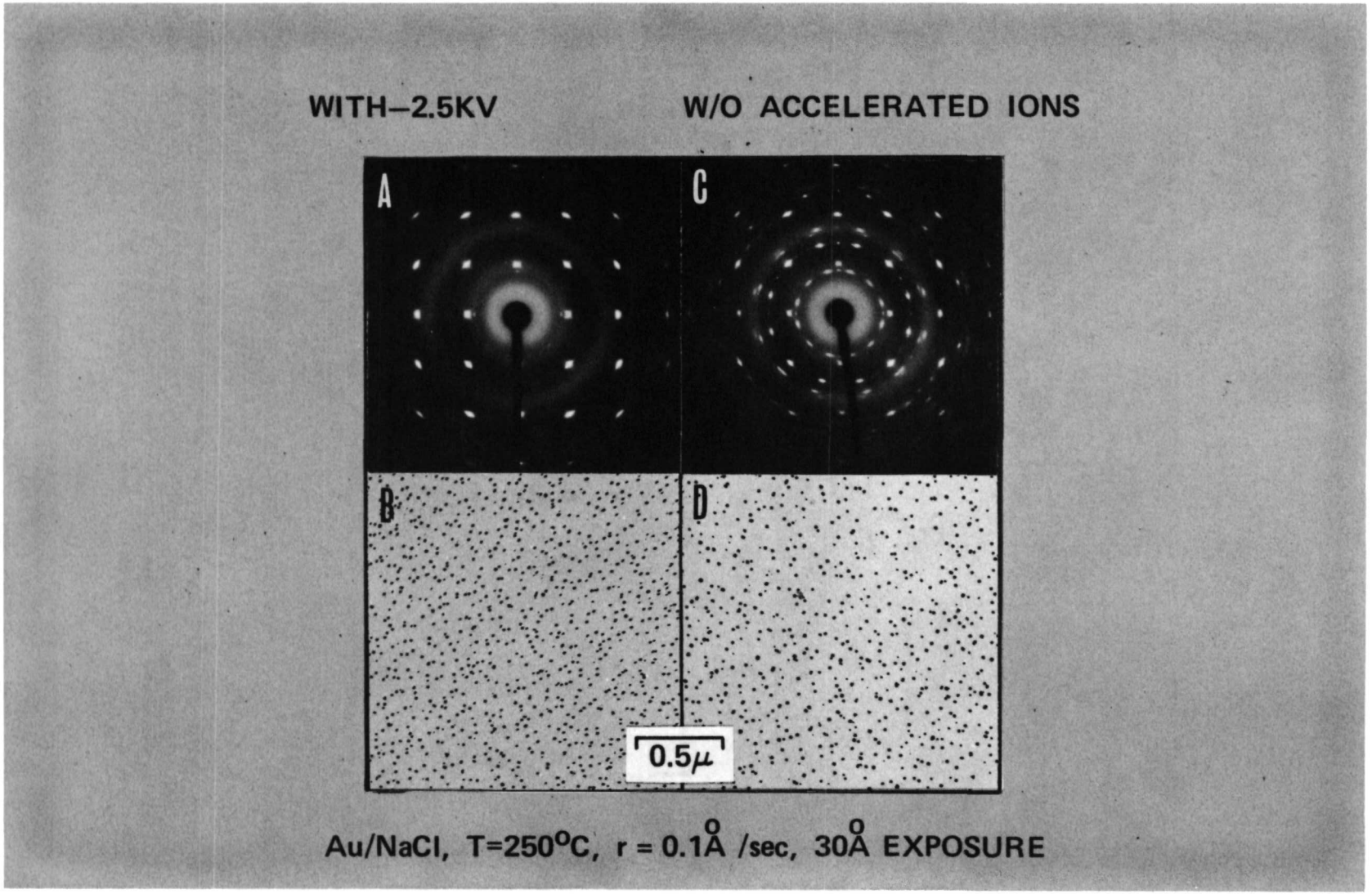
WITH–2.5KV
W/O ACCELERATED IONS
A
C
B
D
0.5μ
Au/NaCl, T=250°C, r = 0.1Å /sec, 30Å EXPOSURE

Figure 19.

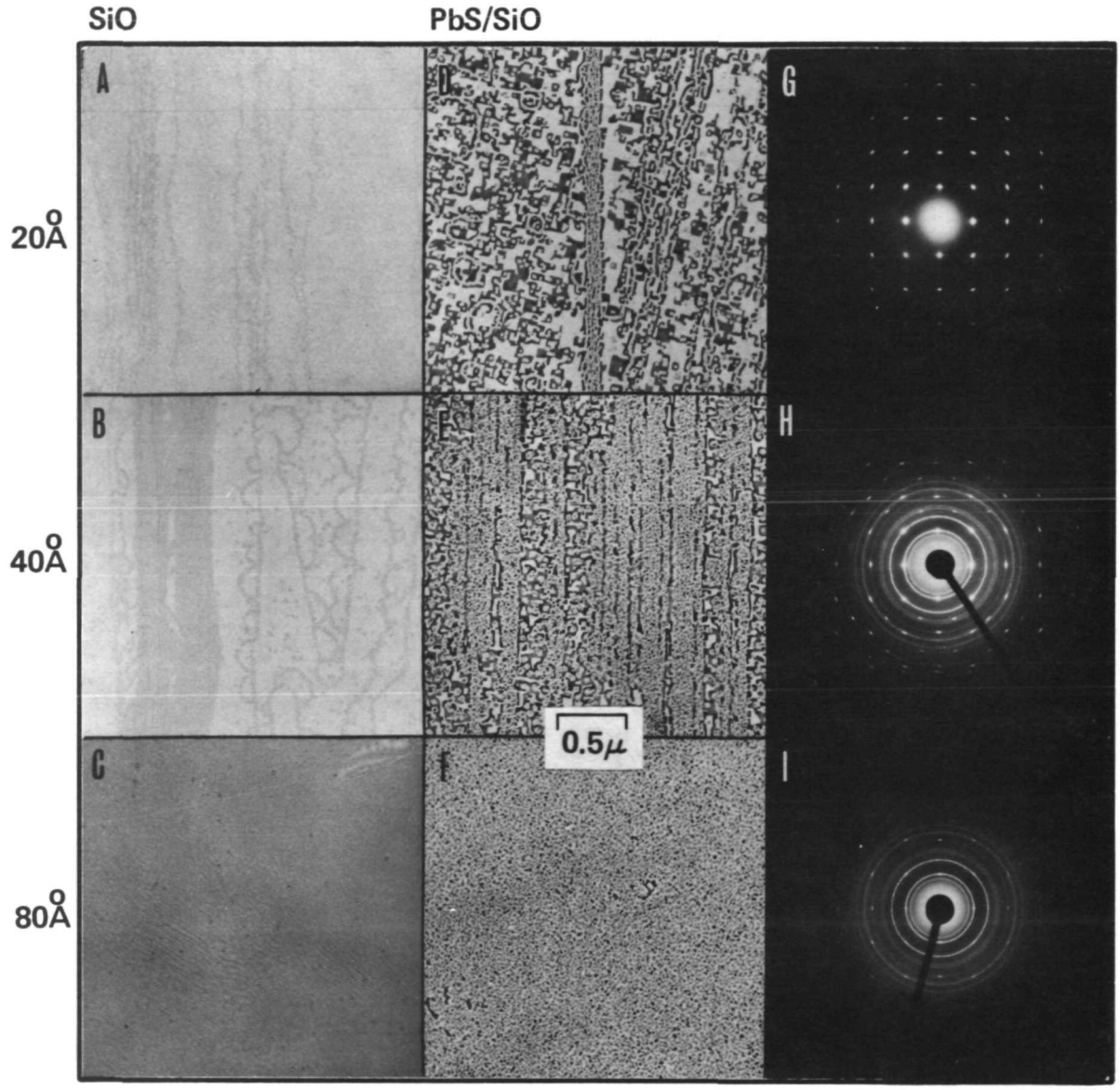

PbS GROWN ON NaCl WITH AN INTERMEDIATE LAYER OF SiO

Figure 20.

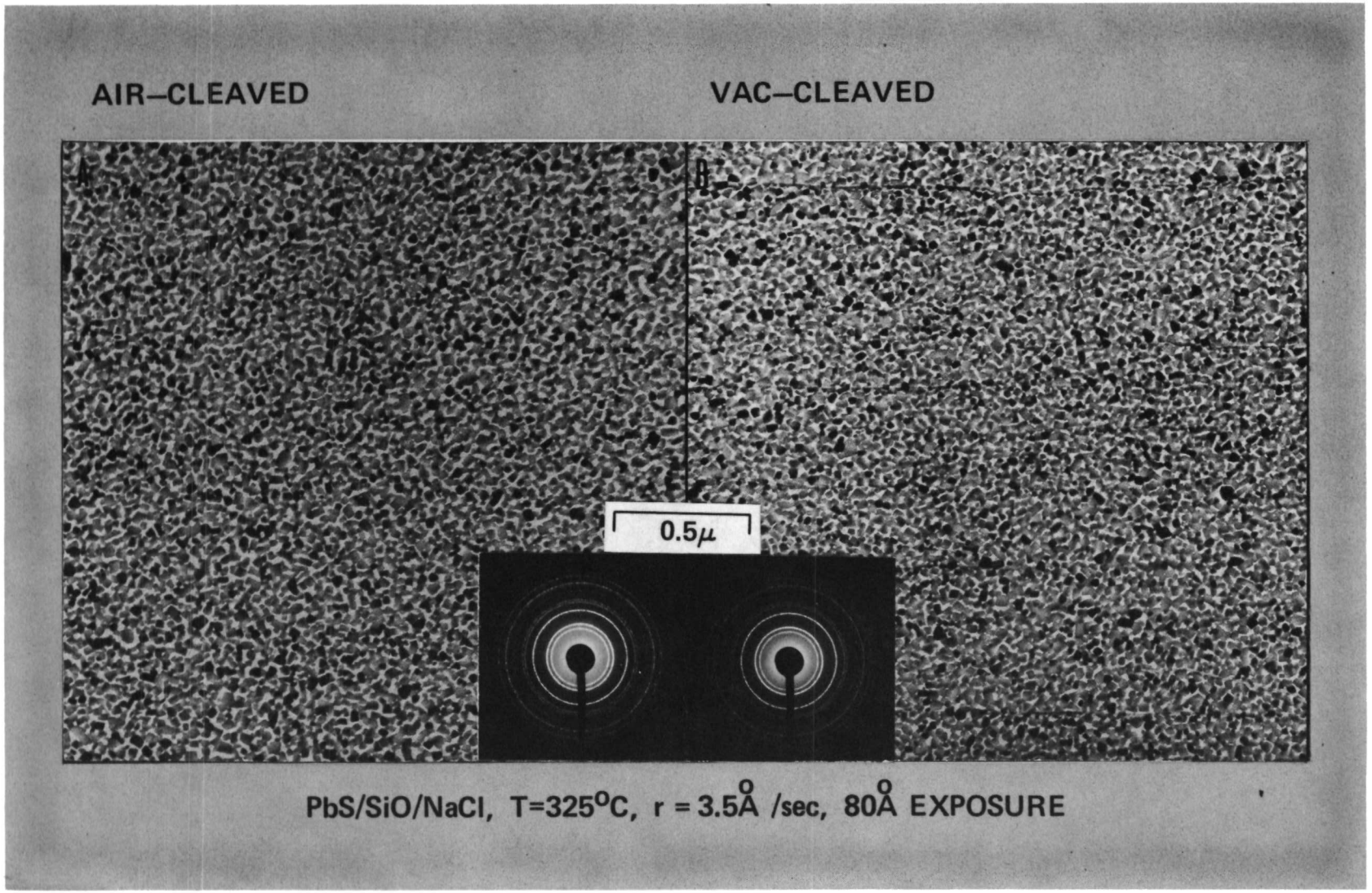
AIR–CLEAVED
VAC–CLEAVED
A
B
0.5μ
PbS/SiO/NaCl, T=325°C, r = 3.5Å /sec, 80Å EXPOSURE

Figure 21.

NATIONAL AERONAUTICS AND SPACE ADMINISTRATION
WASHINGTON, D.C. 20546

OFFICIAL BUSINESS
PENALTY FOR PRIVATE USE $300

SPECIAL FOURTH-CLASS RATE
BOOK

POSTAGE AND FEES PAID
NATIONAL AERONAUTICS AND
SPACE ADMINISTRATION
451

U.S.MAIL

POSTMASTER : If Undeliverable (Section 158 Postal Manual) Do Not Return

"The aeronautical and space activities of the United States shall be conducted so as to contribute . . . to the expansion of human knowledge of phenomena in the atmosphere and space. The Administration shall provide for the widest practicable and appropriate dissemination of information concerning its activities and the results thereof."

—NATIONAL AERONAUTICS AND SPACE ACT OF 1958

NASA SCIENTIFIC AND TECHNICAL PUBLICATIONS

TECHNICAL REPORTS: Scientific and technical information considered important, complete, and a lasting contribution to existing knowledge.

TECHNICAL NOTES: Information less broad in scope but nevertheless of importance as a contribution to existing knowledge.

TECHNICAL MEMORANDUMS: Information receiving limited distribution because of preliminary data, security classification, or other reasons. Also includes conference proceedings with either limited or unlimited distribution.

CONTRACTOR REPORTS: Scientific and technical information generated under a NASA contract or grant and considered an important contribution to existing knowledge.

TECHNICAL TRANSLATIONS: Information published in a foreign language considered to merit NASA distribution in English.

SPECIAL PUBLICATIONS: Information derived from or of value to NASA activities. Publications include final reports of major projects, monographs, data compilations, handbooks, sourcebooks, and special bibliographies.

TECHNOLOGY UTILIZATION PUBLICATIONS: Information on technology used by NASA that may be of particular interest in commercial and other non-aerospace applications. Publications include Tech Briefs, Technology Utilization Reports and Technology Surveys.

Details on the availability of these publications may be obtained from:

SCIENTIFIC AND TECHNICAL INFORMATION OFFICE

NATIONAL AERONAUTICS AND SPACE ADMINISTRATION

Washington, D.C. 20546